Faraday Discussions

Accepted Manuscript

Faraday Discussions

Royal Society of Chemistry

ROYAL SOCIETY OF CHEMISTRY

www.rsc.org/faraday_d

Single-Molecule Spectroscopy and Imaging Over the Decades

W. E. Moerner, Yoav Shechtman, and Quan Wang

Department of Chemistry

Stanford University, Stanford, California 94305 USA

Abstract

As of 2015, it has been 26 years since the first optical detection and spectroscopy of single molecules in condensed matter. This area of science has expanded far beyond the early low temperature studies in crystals to include single molecules in cells, polymers, and in solution. The early steps relied upon high-resolution spectroscopy of inhomogeneously broadened optical absorption profiles of molecular impurities in solids at low temperatures.   Spectral fine structure arising directly from the position-dependent fluctuations of the number of molecules in resonance led to the attainment of the single-molecule limit in 1989 using frequency-modulation laser spectroscopy. In the early 1990's, a variety of fascinating physical effects were observed for individual molecules, including imaging of the light from single molecules as well as observations of spectral diffusion, optical switching and the ability to select different single molecules in the same focal volume simply by tuning the pumping laser frequency. In the room temperature regime, researchers showed that bursts of light from single molecules could be detected in solution, leading to imaging and microscopy by a variety of methods. Studies of single copies of the green fluorescent protein also uncovered surprises, especially the blinking and photoinduced recovery of emitters, which stimulated further development of photoswitchable fluorescent protein labels. All of these early steps provided important fundamentals underpinning the development of super-resolution microscopy based on single-molecule localization and active control of emitting concentration. Current thrust areas include extensions to three-dimensional imaging with high precision, orientational analysis of single molecules, and direct measurements of photodynamics and transport properties for single molecules trapped in solution by suppression of Brownian motion. Without question, a huge variety of studies of single molecules performed by many talented scientists all over the world have extended our knowledge of the nanoscale and microscopic mechanisms previously hidden by ensemble averaging.

1. Introduction

It has now been more than 25 years since the first experiment demonstrating optical detection and spectroscopy of single molecules in a condensed phase [1]. Single-molecule spectroscopy (SMS) allows *exactly one* molecule hidden deep within a crystal, polymer, or cell to be observed via optical excitation of the molecule of interest (Fig. 1a). This represents detection and spectroscopy at the ultimate sensitivity level of $\sim 1.66 \times 10^{-24}$ moles of the molecule of interest (1.66 yoctomole), or a quantity of moles equal to the inverse of Avogadro's number. Detection of the single molecule of interest must be done in the presence of billions to trillions of solvent or host molecules. To achieve this, a light beam (typically a laser) is used to pump an electronic transition of the one molecule resonant with the optical wavelength (Fig. 1b), and it is the interaction of this optical radiation with the molecule that allows the single molecule to be detected. Successful experiments must meet the requirements of (a) guaranteeing that only one molecule is in resonance in the volume probed by the laser, and (b) providing a signal-to-noise ratio (SNR) for the single-molecule signal that is greater than unity for a reasonable averaging time.

Why are single-molecule methods now regarded as a critical part of modern physical chemistry, chemical physics, and biophysics? By removing ensemble averaging, it becomes possible to directly measure distributions of behavior to explore hidden heterogeneity, a property that would be expected in complex environments. In the time domain, the ability to optically sense internal states of one molecule and the transitions among them allows measurement of hidden kinetic pathways and the detection of rare intermediates. Because typical single-molecule labels behave like tiny light sources roughly 1-2 nm in size and can report on their immediate local environment, single-molecule studies provide a new window into the nanoscale with intrinsic access to time-dependent changes.

The basic principles of single-molecule optical spectroscopy and imaging have been the subject of many reviews [2,3,4,5,6,7,8,9,10,11,12] and books [13,14,15,16]. In this introductory paper, key ideas are summarized, starting from the early steps at low temperatures arising from explorations of spectral hole-burning as a method to achieve frequency domain optical storage. Some of the surprising physical effects first observed at low temperatures will then be described, followed by a short overview of the key early steps to achieve room temperature single-molecule detection, but the extremely wide range of applications which have been demonstrated can only be presented in a list. One relatively new advance, super-resolution optical microscopy, can be achieved by single-molecule imaging and localization in situations where the emitting concentration is held to low levels [17,18,19]. Finally, selected recent research thrusts in single-molecule imaging and tracking as well as trapping in solution will be summarized.
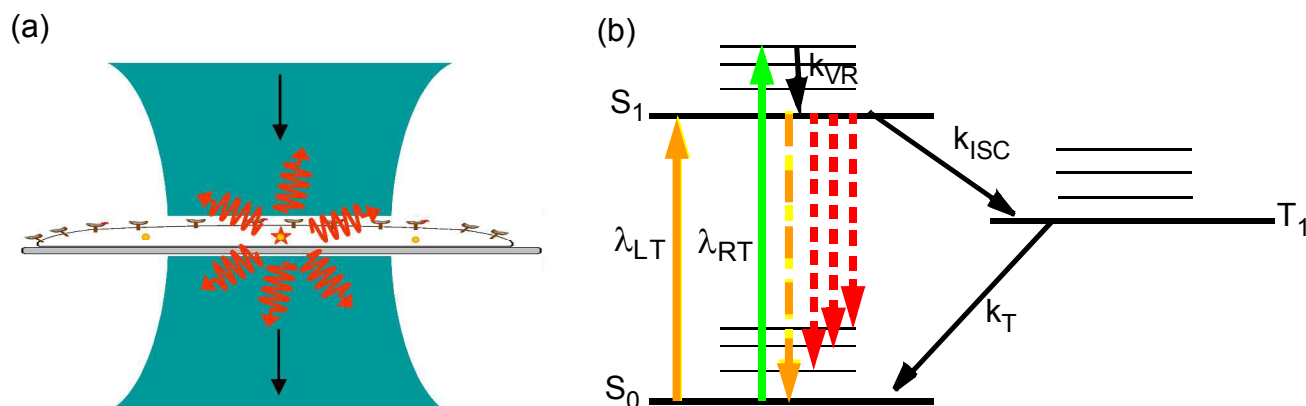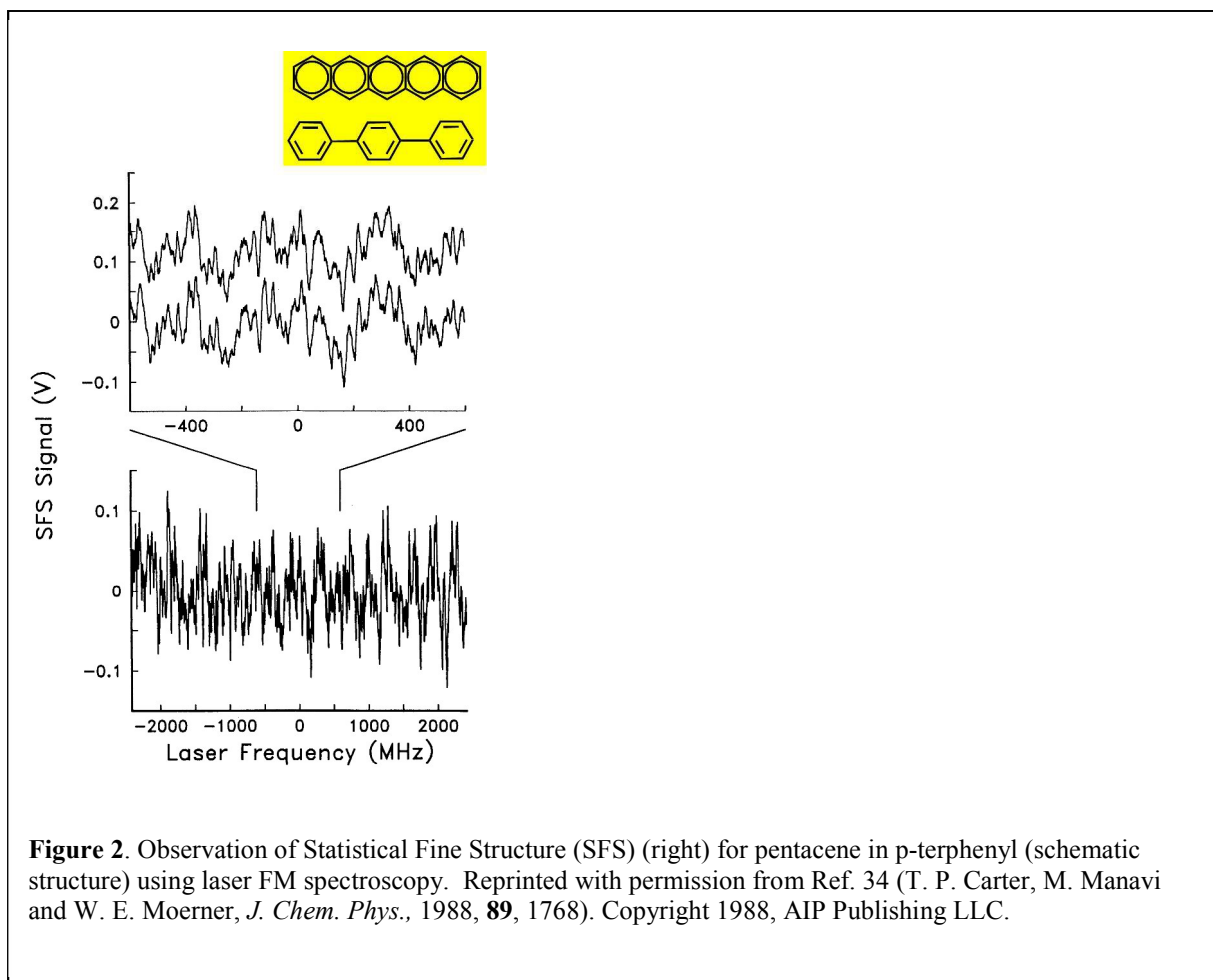
Figure 1. (a) Schematic of a focused optical beam pumping a single resonant molecule in a cell or other condensed phase sample. The molecule may emit fluorescence or its presence may be detected by carefully measuring the transmitted beam. (b) Typical energy level scheme for single-molecule spectroscopy showing the interaction with the pumping light. S_0, ground singlet state; S_1, first excited singlet; T_1, lowest triplet state or other intermediate state. For each electronic state, several levels in the vibrational progression are shown. Typical low-temperature studies use wavelength λ_{LT} to pump the dipole-allowed (0-0) transition, while at room temperature shorter wavelengths λ_{RT} which pump vibronic sidebands are more common. Fluorescence emission shown as dotted lines originates from S_1 and terminates on various vibrationally excited levels of S_0 or S_0 itself. Molecules are typically chosen to minimize entry into dark states such as the triplet state (illustrated), although this or other dark processes can lead to blinking useful in super-resolution microscopy. The intersystem crossing or intermediate production rate is k_{ISC}, and the triplet decay rate is k_T.

1.1 Initial Steps Using Low-Temperature, High-Resolution Spectroscopy in Solids

In the 1970's and 1980's, high-resolution optical spectroscopy of impurities and defects in solids was a major field of chemical and physical research. One goal of this work was to measure the true homogeneous width of the zero phonon, purely electronic transition of molecules in solids. However, these zero-phonon lines were so narrow in frequency space that they became hidden in the broad distribution of resonance frequencies caused by the random strains and stresses present in solids, and the absorption lines were known to be inhomogeneously broadened [20-22]. It is for this reason that much research in the 1970's and 1980's was devoted to methods like fluorescence line narrowing (FLN) [23, 24] and transient spectroscopies such as free induction decay, optical nutation, and photon echoes [25-27]. While these were all powerful methods with advantages and disadvantages, there was another method to assess the homogeneous width under certain circumstances, persistent spectral hole-burning[28]. This effect produced marks or dips in absorption, termed "holes," in an inhomogeneous line caused by photochemical changes [29] or photophysical changes [30] in the nearby environment. One of us (WEM), was employed at IBM Research in San Jose, California, where hole-burning was being developed for an optical storage scheme called "frequency-domain optical storage" [31]. Happily, it was important at this industrial research lab to not only develop new materials and methods for spectral hole-burning storage

4

(See various chapters in Ref. [28]), but it was also a key goal to define and understand fundamental limits of signal-to-noise ratio, etc. [32]. Due to unavoidable number fluctuations in the actual number of molecules present in any spectral interval, there should exist a "spectral roughness" on an inhomogeneous absorption profile scaling as the square root of the number of molecules in resonance (i.e., the number of molecules per homogeneous width, N_H). We named this effect "statistical fine structure" (SFS), and the *relative* size of SFS should scales as $1/\sqrt{N_H}$, while the absolute root-mean-square (rms) size of the fine structure should grow as $\sqrt{N_H}$. Surprisingly, prior to the late 1980's, SFS had not been detected.

In 1987, SFS was observed for the first time by Moerner and Carter [33,34], using a powerful zero-background optical absorption technique, laser frequency-modulation (FM) spectroscopy invented by Gary C. Bjorklund earlier [35,36]. FM spectroscopy (FMS) probes the sample with a phase-modulated laser beam which produces two out-of-phase sidebands on the laser carrier.

Figure 2. Observation of Statistical Fine Structure (SFS) (right) for pentacene in p-terphenyl (schematic structure) using laser FM spectroscopy. Reprinted with permission from Ref. 34 (T. P. Carter, M. Manavi and W. E. Moerner, *J. Chem. Phys.,* 1988, **89**, 1768). Copyright 1988, AIP Publishing LLC.

When a narrow spectral feature is present, the imbalance in the laser sidebands leads to amplitude modulation in the detected photocurrent at the modulation frequency. A key feature of the method is that it senses only the deviations of the absorption from the average value, so that detection of SFS could be easily accomplished, but only if a test sample was chosen with

minimal spectral hole-burning so that the shape of the inhomogeneous profile could be measured without disturbance from the scanning. The choice of sample was critical: pentacene dopant molecules in a transparent p-terphenyl crystal (Fig. 2), in which spectral hole-burning was very weak. In the lower traces of Fig. 2, SFS is the repeatable spectral roughness seen in the lower trace, a small part of which is shown in the upper panel, with two repeated acquisitions – this is not time-dependent noise! SFS is clearly an unusual spectral feature, in that its (rms) size depends not upon the total number of resonant molecules, but rather upon the square root of the number.
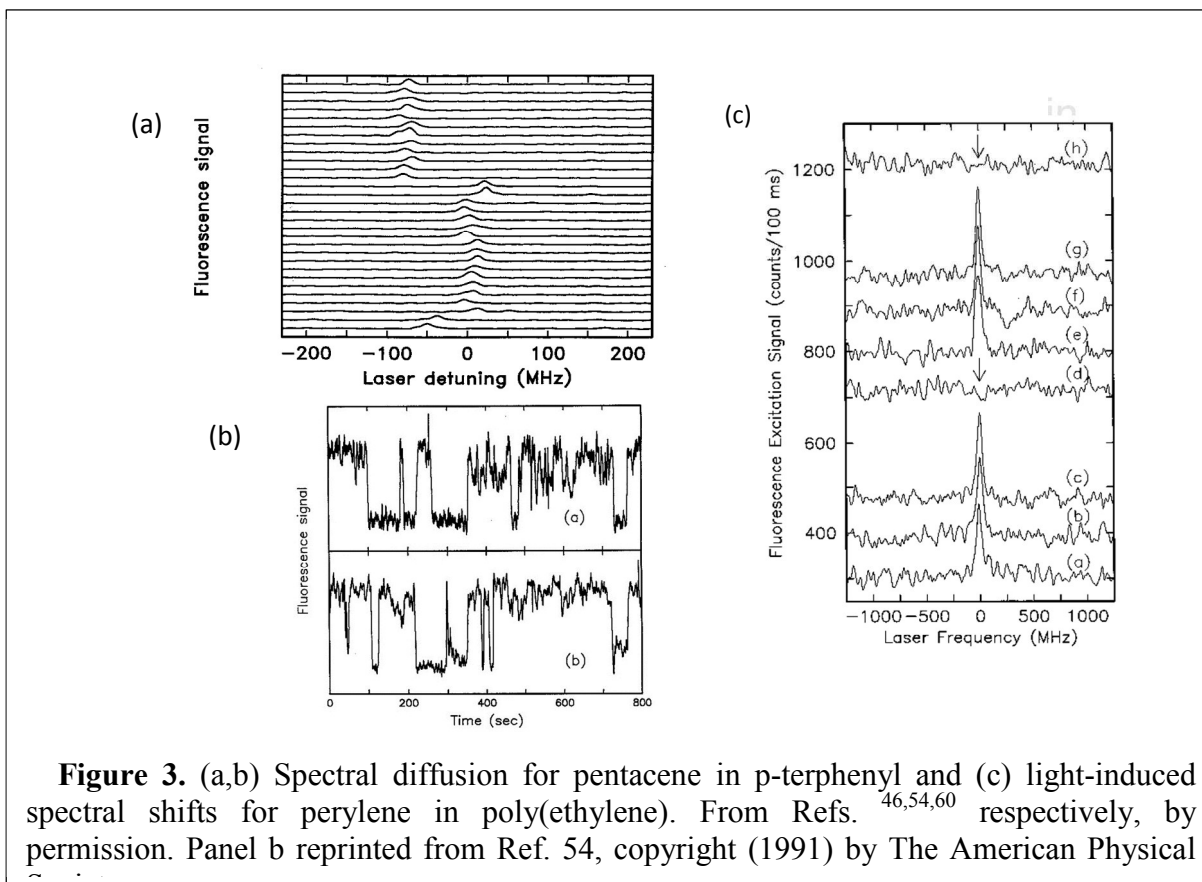
With the detection of SFS in hand, it became possible to push on toward single-molecule detection. The first SMS experiments in 1989 by Moerner and Kador utilized either of two powerful double-modulation FMS absorption techniques, laser FMS with Stark secondary modulation (FM-Stark) or FMS with ultrasonic strain secondary modulation (FM-US) [1, 37]. Secondary modulation was required in order to remove the effects of residual amplitude modulation produced by the imperfect phase modulator[38]. The optical absorption experiments on pentacene in p-terphenyl indeed showed that this material has sufficiently inefficient spectral hole-burning to make it a useful model system for single-molecule studies. In 1990, Michel Orrit and Jacky Bernard produced a further critical advance: they demonstrated that sensing the optical absorption by detection of the emitted fluorescence produces superior signal-to-noise if the emission is collected efficiently and the scattering sources are minimized [39]. Due to its relative simplicity, subsequent experiments have almost exclusively used this method, which is also called "fluorescence excitation spectroscopy." In fluorescence excitation, a tunable narrowband single-frequency laser is scanned over the absorption profile of the single molecule, and the presence of absorption is detected by measuring the fluorescence emitted to long wavelengths, away from the laser wavelength itself. The method is often background-limited, and it requires the growth of ultrathin crystal clear sublimed flakes to reduce the scattering signals that could arise from the p-terphenyl crystal, but it does not suffer from the difficult tradeoff between SNR and optical broadening that occurred with FM spectroscopy.

With the ability to detect single molecules in crystals and polymers, in the early 1990's many investigators all over the world jumped into the field in order to take advantage of the extremely narrow optical absorption lines available at low temperatures and the removal of ensemble averaging, two of the largest motivations for the study of single molecules[13]. Investigations were sometimes directed at specific observations of particular processes like the Stark effect [40], two-level system dynamics [41], or polarization effects [42] to name a few. At other times experiments were performed simply to observe, because surprises would be expected when a new regime is first explored. The great body of work done is too large to review here, and the reader is referred to selected texts [13, 28] and selected review articles [2-5, 43-45] for more information. The Moerner group of postdocs and collaborators completed a wide array of experiments, including measurements of the lifetime-limited width, temperature-dependent dephasing, and optical saturation effects[46, 47], photon antibunching correlations [48], vibrational spectroscopy [49-51], magnetic resonance of a single molecular spin [52], and near-field spectroscopy [53]. Some

experiments have particular relevance for super-resolution microscopy and will be discussed next.

1.2. Surprises from Single-Molecule Spectroscopy: Blinking and Photocontrol

During the early SMS studies on pentacene in p-terphenyl, an unexpected phenomenon appeared: resonance frequency shifts of individual pentacene molecules in a crystal at 1.5 K [46, 54], mentioned briefly by Orrit [39]. We called this effect "spectral diffusion" due to its close relationship to similar spectral-shifting behavior long postulated for optical transitions of impurities in amorphous systems [55]. Here, spectral diffusion means changes in the center (resonance) frequency of a probe molecule due to configurational changes in the nearby host which affect the frequency of the electronic transition via guest-host coupling. Ambrose and Moerner observed this at the single-molecule level as shown in Fig.3a, which displays a sequence of fluorescence excitation spectra of a single pentacene molecule in p-terphenyl taken as fast as allowed by the available SNR, every 3 s. The spectral shifting or hopping of this molecule from one resonance frequency to another from scan to scan is clearly evident. Now if the laser frequency is held fixed near the molecular absorption, then the molecule appears to blink on and off as it jumps into and out of resonance (Fig. 3b, at two power levels). Due to the lack of power dependence on the rate, these spontaneous processes suggested that there are two-level systems available in the host matrix which can undergo thermally induced transitions even at these low temperatures. One possible source for the tunneling states in this crystalline system could be discrete torsional librations of the central phenyl ring of the nearby p-terphenyl molecules about the molecular axis. The p-terphenyl molecules in a domain wall between two twins or near lattice defects may have lowered barriers to such central-ring tunneling motions, a useful model proposed by Jim Skinner and co-workers [56-58]. These studies illustrate the power of SMS in probing details of the local nanoenvironment and the importance of theoretical insight to further understanding. Spectral shifts of single-molecule lineshapes were observed not only for certain crystalline hosts, but also for essentially all polymers studied, and even for polycrystalline Shpol'skii matrices [59]. This is a dramatic example of the heterogeneity that was uncovered by the single-molecule studies.

Figure 3. (a,b) Spectral diffusion for pentacene in p-terphenyl and (c) light-induced spectral shifts for perylene in poly(ethylene). From Refs. [46,54,60] respectively, by permission. Panel b reprinted from Ref. 54, copyright (1991) by The American Physical

In addition, Basché and Moerner observed light-driven shifts in absorption frequency for perylene dopant molecules in poly(ethylene), in which the rate of the process clearly increased with increases in laser intensity [60, 61], Fig. 3c. This photoswitching effect may be called "single-molecule hole-burning" by analogy with the earlier hole-burning literature [28]; however, since only one molecule is in resonance with the laser, the absorption line simply disappears. Subtraces (a), (b), and (c) show three successive scans of one perylene molecule. After subtrace (c) the laser was tuned into resonance with the molecule, and at this higher irradiation fluence, eventually the fluorescence signal dropped, that is, the molecule apparently switched off. Subtrace (d) was then acquired, which showed that the resonance frequency of the molecule apparently shifted by more than +/-1.25 GHz as a result of the light-induced change in the nearby environment. Surprisingly, this effect was reversible for a good fraction of the molecules: a further scan some minutes later (subtrace (e)) showed that the molecule returned to the original absorption frequency. After subtrace (g) the molecule was photoswitched again and the whole sequence could be repeated many times, enabling us to measure the Poisson kinetics of this process from the waiting time before a spectral shift [61]. Optical modification of single-molecule spectra not only provided a unique window into the photophysics and low-temperature dynamics of the amorphous state, this effect presaged another area of current interest at room temperature:

photoswitching of single molecules between emissive and dark forms is a powerful tool currently being used to achieve super-resolution imaging (*vide infra*).

2. Room Temperature Studies of Single Molecules

Soon after the first low-temperature experiments, studies began of single molecules at room temperature. A selection of crucial early milestones are described in Table 1.

Solution: Correlation functions	Fluorescence Correlation Spectroscopy (FCS): [62-65,66,67]; …	1972…
	Autocorrelation detected from 1 fluorophore or less in the volume: [68]	1990
Solution: Single bursts	Multichromophore emitter bursts (phycoerythrin): [69]	1989
	Single bursts of fluorescence from 1 fluorophore: [70,71];…	1990…
Solution and surface	Single antibody with multiple (~80-100) labels: [72]	1976
Near-Field Scanning Optical Microscopy	Imaging a single fluorophore: [73,74,75]	1993…
Confocal imaging	Single molecule in a polymer: [76]; …	1996
Widefield, single fluorophore imaging	*In vitro*, single myosin on actin: [77]	1995
	Cell membrane, single-lipid tracking with super-localization: [78]	1996

Table 1. Room temperature milestones of single-molecule detection and imaging.

Early steps arose out of the development of "fluorescence correlation spectroscopy" (FCS) [63, 64], a large body of work which has been extensively reviewed in [79-81]. The method depends upon the fluctuations in emission from a tightly focused spot in solution arising from passage of molecules diffusing through a laser beam. Autocorrelation analysis of the fluorescence provides a window into a variety of dynamical effects on time scales less than the transit time on the order of 1-10 ms. The contrast ratio of the autocorrelation degrades at high concentrations but improves at low, and in 1990 correlation functions were recorded from concentrations so low that much less than one molecule was in the probe volume [68]. The passages of many single molecules must be averaged; it is impossible to study one and the same molecule for a long time with FCS – for a solution to this, see Section 5.

A crucial advance occurred in 1990, when the Keller lab at Los Alamos used a carefully designed hydrodynamic flow to reduce the volume producing interfering background signals and directly detected the individual fluorescence bursts as individual single rhodamine 6G molecules passed through the focus[70]. This was a key step in reducing backgrounds, but there is great value
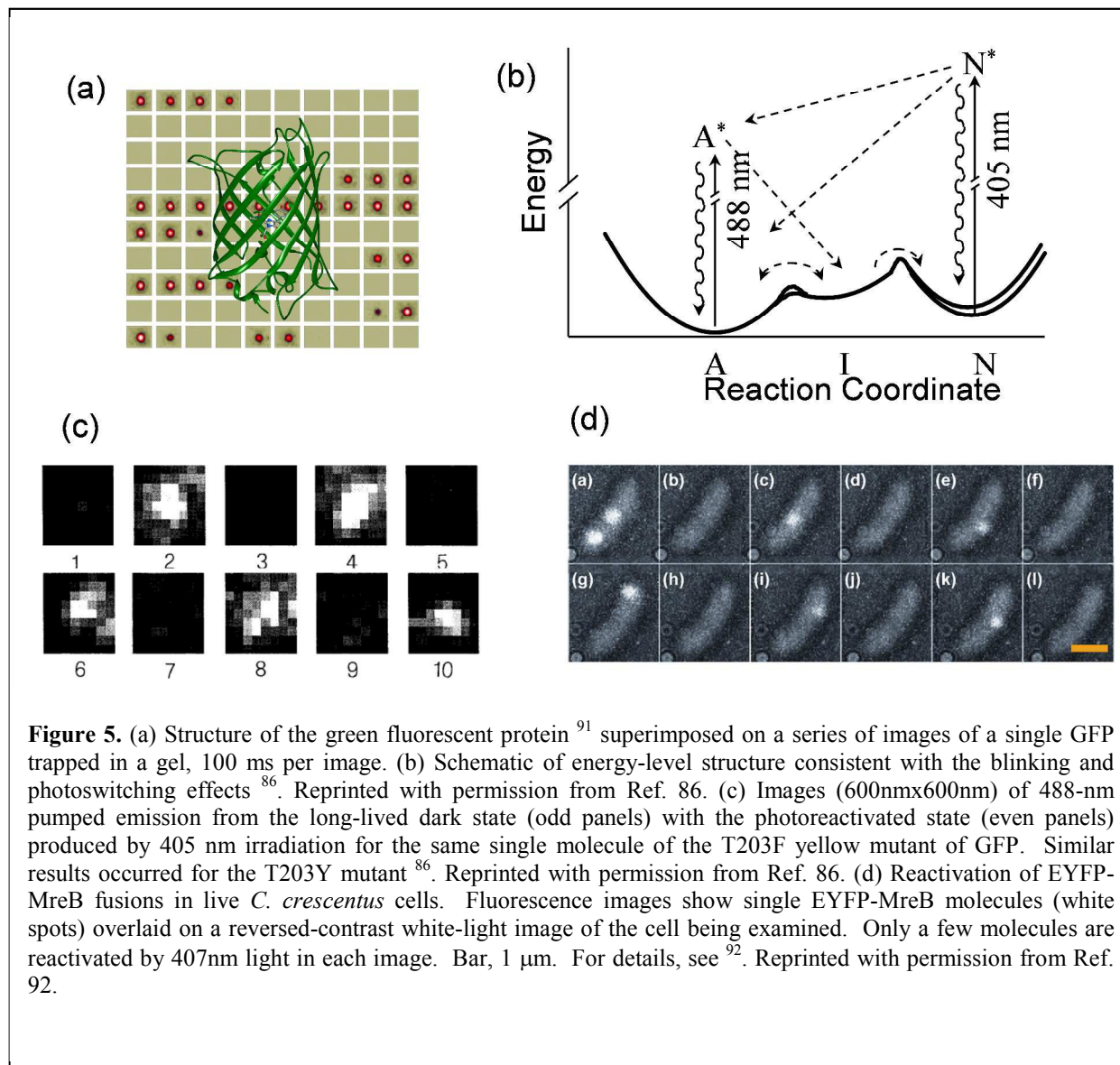
in being able to watch the same single molecule for extended periods, measuring signal strength, lifetime, polarization, fluctuations, and so on, all as a function of time and with the express purpose of directly detecting any heterogeneity from molecule to molecule. Hirschfeld reported detection of a single antibody with 80-100 fluorophores in a short report much earlier in 1976 [72], but severe photobleaching and the optical apparatus available at the time limited further work.

A further milestone occurred in 1993 when single-molecule imaging at room temperature was demonstrated using near-field scanning optical microscopy (NSOM) [73,74,75]. It was subsequently demonstrated that with careful sample preparation and optimal detection, single molecules could be imaged with far field techniques such as confocal microscopy [76], wide-field epifluorescence, and total internal reflection fluorescence microscopies [77]. Of particular importance for cell biology applications, in 1996 Schmidt et al. explored the diffusion of single labeled lipids on a cell surface [78]. The explosion of methods allowing single-molecule detection and imaging has led to a wealth of exciting research in this area, with advances far too numerous to review comprehensively [7, 82, 83], and two sets of Nobel Conference Proceedings have appeared [84, 85].

- Förster resonance energy transfer
- Polarization microscopy
- Photon antibunching
- Counting subunits (stoichiometry)
- Probing metallic nanoantenna structures for electromagnetic enhancements
- Vibrational mode spectra
- Stark effects
- Optically detected magnetic resonance
- Surface-enhanced Raman scattering
- Detection without fluorescence at room T
- Force spectroscopy (optical tweezers, magnetic tweezers, AFM…)
- Nanoscale materials studies: polymers, crystals, glasses
- Biophysics and Cell Biology – HUGE number of applications: enzymes, signaling, molecular motors, actin bands, DNA processing and dynamics, RNA, gene expression, chaperonins, viral entry, photosynthetic antenna proteins, …, …
- Tracking and trapping single molecules in solution and in cells
- New fluorophores and fluorophore dynamics
    - Blinking effects
    - Optical and chemical control of single molecule emission
    - Color centers in diamond
- Nanoparticles: metals, semiconductors, polymers

Figure 4. A selection from the huge variety of single-molecule methods and applications over the decades – with apologies for possible omission.

During the years since the 1990's, a stunning array of single-molecule experiments have been performed in many environments to explore biophysics, polymer dynamics, cellular processes, and dynamics. Reviewing all these studies is impossible at this time, as is properly referencing all the work that has been done, so in Fig. 4, a partial list is provided. The textbooks and book chapters referenced at the start of this paper should be consulted for details. One particular imaging study in 1997 deserves a bit of additional mention: Dickson and Moerner used the water-filled pores of poly(acrylamide) gels to achieve optical imaging of single copies of a green fluorescent protein (GFP) mutant using total-internal-reflection fluorescence microscopy[86]. As was the case with the first low-temperature studies, an unexpected surprise occurred: the first example of blinking and optical switching of a single fluorescent protein. The experiments utilized two yellow-emitting GFP mutants (S65G/S72A/T203Y denoted "T203Y" and S65G/S72A/T203F denoted "T203F"), which differ only by the presence of a hydroxyl group near the chromophore, both of which are quite similar to the currently widely used enhanced yellow fluorescent protein EYFP (S65G/V68L/S72A/T203Y). Figure 5a illustrates the blinking

Figure 5. (a) Structure of the green fluorescent protein [91] superimposed on a series of images of a single GFP trapped in a gel, 100 ms per image. (b) Schematic of energy-level structure consistent with the blinking and photoswitching effects [86]. Reprinted with permission from Ref. 86. (c) Images (600nmx600nm) of 488-nm pumped emission from the long-lived dark state (odd panels) with the photoreactivated state (even panels) produced by 405 nm irradiation for the same single molecule of the T203F yellow mutant of GFP. Similar results occurred for the T203Y mutant [86]. Reprinted with permission from Ref. 86. (d) Reactivation of EYFP-MreB fusions in live *C. crescentus* cells. Fluorescence images show single EYFP-MreB molecules (white spots) overlaid on a reversed-contrast white-light image of the cell being examined. Only a few molecules are reactivated by 407nm light in each image. Bar, 1 μm. For details, see [92]. Reprinted with permission from Ref. 92.

behavior: a single molecule emits frame after frame but then turns off, only to turn on again after a time in a stochastic fashion. This blinking behavior likely results from transformations between at least two states of the chromophore (A and I, Fig. 5b), only one of which (A) is capable of being excited by the 488 nm pumping laser and producing fluorescence. Additionally, a much longer-lived dark state N is also accessible. Thermally stable in the dark for many minutes, this long-lived dark state is not permanently photobleached, but can be excited at 405 nm to regenerate the original fluorescent state as shown in the sequence of images in Fig. 5c. This means that the protein can be used as an emitting label until it enters the long-lived dark state, and it can be photo-reactivated back to the emissive form with the 405 nm light, a reversal of the apparent photobleaching. This can occur many times for the same single molecule. Switching and blinking effects also occur for single fluorescent protein fusions expressed in bacteria as shown in Fig. 5d. These effects, and similar effects in a variety of other engineered photoswitchable fluorescent proteins (such as Kaede [87], PA-GFP [88], EosFP [89], and DRONPA [90]), can be utilized for super-resolution imaging [17, 19], to be described next.

3. Super-Resolution Imaging Based on Single Molecules

One continuing driving force in single-molecule fluorescence studies is the study of biomolecules, *in vitro* and *in vivo* [82]. As is well-known, biological fluorescence microscopy depends upon a variety of labeling techniques to light up different structures in cells, but the price often paid for using visible light is the relatively poor spatial resolution compared to x-ray crystallography or electron microscopy. When attempting to image nanoscale structures with visible light, a serious problem arises: fundamental diffraction effects first noted by Abbe in the late 1800's [93] limit the resolution to a dimension of roughly the optical wavelength λ divided by two times the numerical aperture (NA) of the imaging system, $\lambda/(2 \times NA)$. Here resolution means the ability to distinguish two point objects which are closely spaced; when individual molecules are far apart as shown in Fig. 1a, there is no problem imaging them separately. Since the largest values of NA for state-of-the-art, highly corrected microscope objectives are in the range of about 1.3-1.6, the spatial resolution of optical imaging has been limited to about ~200 nm for visible light of 500 nm wavelength.

In recent years, several optical methods have appeared which allow optical microscopy to surpass the diffraction limit to achieve "super-resolution", recognized by the Nobel Prize in Chemistry in 2014. All such methods rely on the use of fluorophores which can have two states: an emissive "on" state and a dark "off" state. One class of methods are based on optical patterning of a depletion beam to turn off molecules whose emission is not desired, as in Stimulated Emission Depletion (STED) microscopy of Stefan Hell and its variants [94]. A related method by Mats Gustafsson (Structured Illumination Microscopy or SIM) uses interfering beams to achieve resolution beyond the diffraction limit [95]. Neither of these methods requires single-molecule sensitivity, so subsequently in this paper we will focus on the methods which do

require single-molecule imaging.
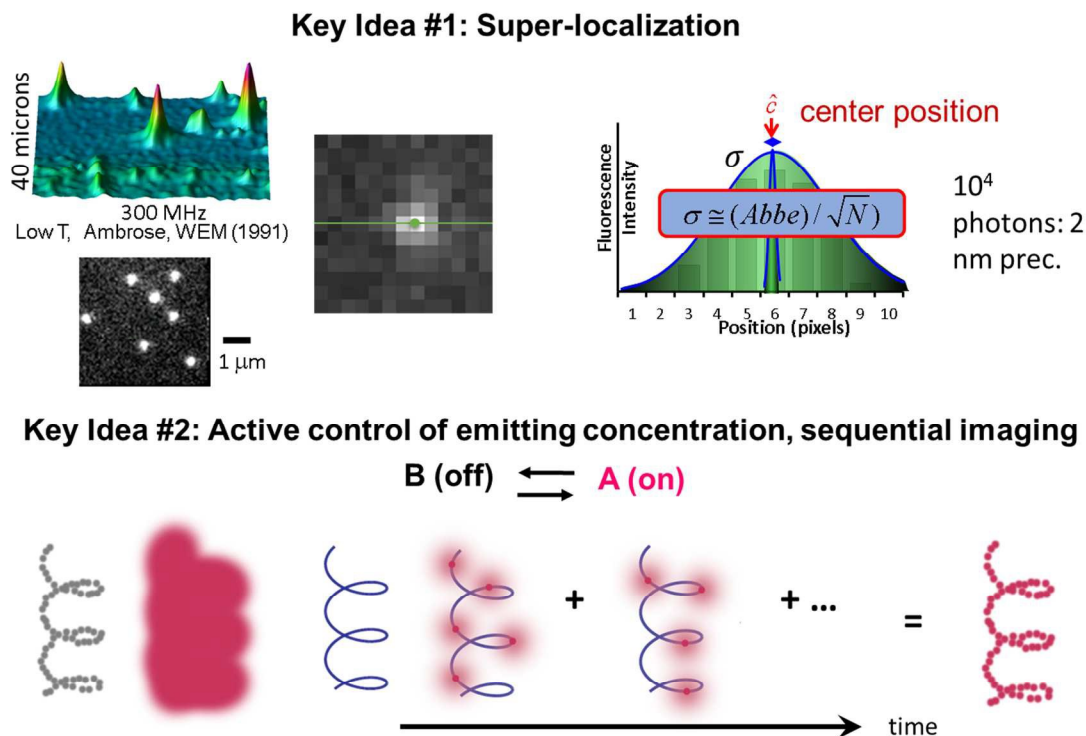
Figure 6. Illustration of the key ideas underlying super-resolution optical microscopy based on single-molecule localization combined with active control of the emitting concentration and sequential imaging.

The basic idea is illustrated in a general way in Fig. 6, which illustrates the two critical ideas. In the first Key Idea, one must be able to super-localize single molecules in an image, which means finding the position of each molecule to a precision better than the diffraction limit. At the upper left of the figure, one of the original low temperature images of single molecules is shown for reference [46]. At room temperature, with a wide-field image of single molecules shown in the white on black panel, the diffraction-limited spots are evident. It is essential to spread out each detected spot on multiple pixels of the camera as shown in the next panel to the right. Then, illustrated by a 1D cross-section at the upper right, the various pixels detect different numbers of photons according to the shape of the point spread-function (PSF) of the microscope. Formally the PSF is an Airy function, but it may be approximated by a Gaussian function for simplicity, especially in the presence of background. The photon numbers detected in the various pixels provide samples of the function, which may be fit mathematically. While the width of this fit is still diffraction-limited with width $\hat{w}$, the estimate of the center position $\hat{c}$ from the fit follows a much narrower error distribution with standard deviation σ, which is generally called the "localization precision." The precision with which a single molecule can be located by digitizing the PSF depends fundamentally upon the Poisson process of photon detection, so the most important variable is the total number of photons N detected above background, with a weaker

dependence on the size of the detector pixels and background [96-98]. The leading dependence of σ is just the Abbe diffraction limit divided by the square root of the number of photons detected in the image. This functional form makes sense, since each detected photon is an estimate of the molecular position, so for N measurements, the precision improves as expected. Super-localization means that if 100 photons are detected, then the precision can approach 20 nm, and so on. Clearly, then, emitters with the largest numbers of emitted photons before photobleaching are preferable. This is a commonly used method for determining the position of single objects from a diffraction-limited image [99], and early applications in biology include determinations of the centroid of large LDL particles[100] or fluorescent beads attached to single myosin motors[101]. Of course, this method also works with single molecules, for example, to track the motion of a single lipid molecule on a cell membrane[78] and many other examples. But super-localization only works for a single molecule far away from its peers, so that the diffraction-limited images do not overlap.

True super-resolution requires the ability to localize single molecules when their PSFs do overlap, and this requires Key Idea #2. The early history of various fledgling approaches to solve this problem is described in Table II of Ref. [102], so here only the general form of the idea is described as shown in the lower part of Fig. 6. The key concept is to actively control the emitting concentration and then sequentially image to obtain the single-molecule positions. A structure has been labeled with many fluorescent labels as shown on the left, but when all are allowed to emit simultaneously, the blurry image results because the many PSFs overlap. The key idea is simply to <u>not</u> allow all the molecules to emit at the same time! Let us suppose that there is some mechanism which allows the emitters to be "On" part of the time and emitting photons (state A), and "Off", or dark, another part of the time (state B), even though the pumping light is still present. The experimenter uses this mechanism to <u>actively control the concentration of emitting molecules to a very low level</u> such that the PSFs do not overlap in any one image. Effectively then, a random small subset of the emitters are in the emissive state. Then using super-localization in one acquired image of the molecules, the positions of those are determined and recorded. Then these molecules are turned off or photobleached, and another subset is turned on, super-localized, etc. In the end, after a number of sequential imaging cycles, many locations on the structure have been sampled using the tiny single-molecule "beacons", and the underlying image is reconstructed in a pointillist fashion to show the detail previously hidden beyond the diffraction limit on the right. In this way, the locations of the single molecule labels are learned by sequential imaging, analogous to time-domain multiplexing.

This idea was first presented by Eric Betzig and his primary collaborator, Harald Hess, in April 2006 at the Frontiers in Live Cell Imaging Conference at the NIH main campus in Bethesda, Maryland. They used the PA-GFP photoactivatable fluorescent proteins of George Patterson and Jennifer Lippincott-Schwartz [88] and other photoswitchable fluorescent proteins as an active control mechanism, terming the method PALM (for PhotoActivated Localization Microscopy)[17]. Light-induced photoactivation of GFP mutant fusions is used to randomly turn on only a few single molecules at a time in fixed cell sections or fixed cells. In their experiment,

individual PSFs were recorded in detail to find their positions to ~ 20 nm, then the emitters were photobleached so that others could be turned on, and so on until many thousands of PSF positions were determined, and a super-resolution reconstruction was produced.

Very quickly after the NIH meeting, a flood of researchers demonstrated super-resolution imaging with single molecules and additional active control mechanisms and additional acronyms. The laboratory of Xiaowei Zhuang utilized controlled photoswitching of small molecule fluorophores for superresolution demonstrations [18](STORM, for STochastic Optical Reconstruction Microscopy). Samuel Hess et al. published a nearly identical approach with an acronym termed F-PALM (Fluorescence PhotoActivation Localization Microscopy) [19], which also utilized a photoactivatable GFP with PSF localization to obtain superresolution. Also in 2006, an alternative approach was reported by the laboratory of Robin Hochstrasser based on accumulated binding of diffusible probes, which are quenched in solution yet de-quench in close proximity of the surface of the object to be imaged [103] (termed PAINT, for Points Accumulation for Imaging in Nanoscale Topography). The method relies upon the photophysical behavior of certain molecules that light up when bound or constrained, and they demonstrated the idea with the twisted intermolecular charge transfer (TICT) of Nile Red [104]. PAINT has advantages that the object to be imaged need not be labeled and that many individual fluorophores are used for the imaging, thus relaxing the requirement on the total number of photons detected from each single molecule.

Other active control mechanisms quickly appeared such as dSTORM[105] (direct STORM), GSDIM (Ground-State Depletion with Intermittent Return)[106], blinking as in BLINK-microscopy [107], SPDM (Spectral Precision Determination Microscopy) [108], and the list goes on. In 2008, Julie Biteen in the Moerner laboratory used the EYFP photorecovery mechanism described above to perform super-resolution imaging in bacteria [92], and an example image is presented below in Fig. 7. There are photochemical methods for single-fluorophore turn-on [109] and even enzymatic methods for turn-on which may be controlled by the concentration of substrate and the enzymatic rate [110]. The experimenter must actively choose some method to control the emitting concentration. Of course, the imaging is still time-sequential, thus this approach is best for quasi-static structures or fixed cells, but significant progress has been made in increasing the imaging speed [111]. Selected reviews may be consulted for additional detail of modern challenges and progress in super-resolution imaging [112-115,116,117-120], and some current thrust areas are described in Section 4.
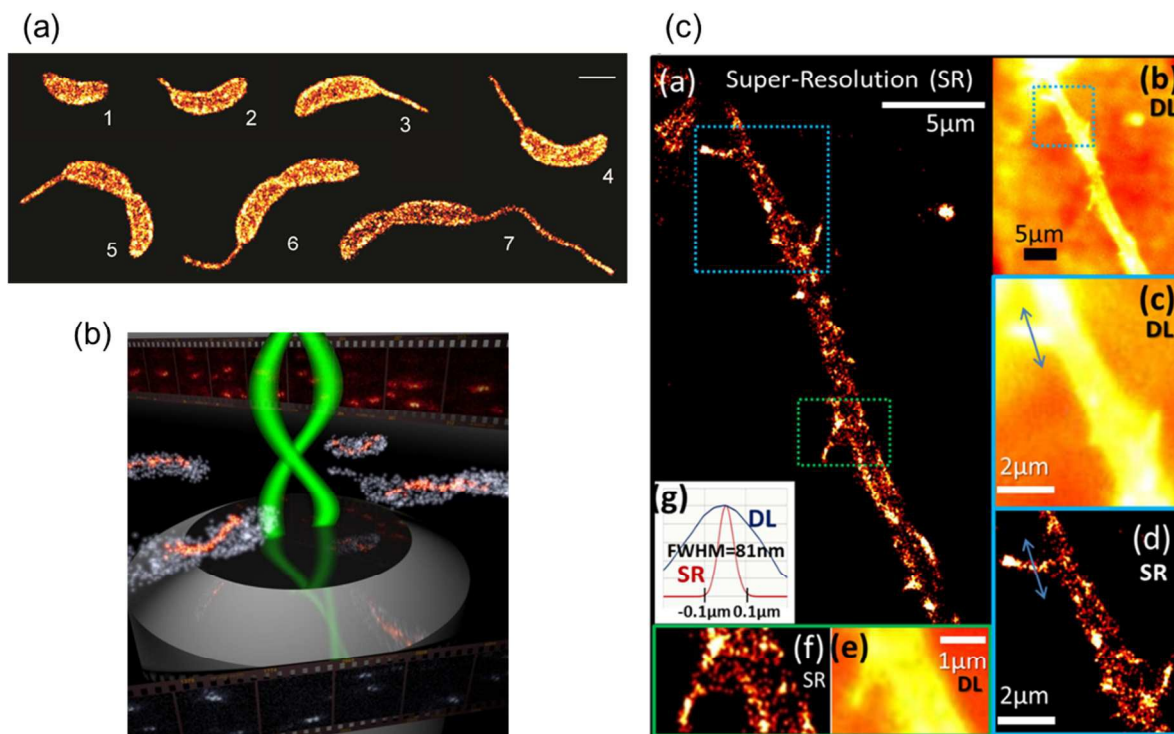
Figure 7. Selected super-resolution images in cells. (a) The cell surface of *Caulobacter crescentus* bacteria. Scale bar = 1 µm. From Ref. 121 by permission. (b) Two-color 3D imaging of the cell surface and a protein fiber-like structure in *Caulobacter*. Wikimedia file Bacteria-3D-Double-Helix.jpg Creative Commons Attribution-Share-Alike 4.0 International license. (c) Super-resolution and diffraction-limited (DL) images of the locations of voltage-gated sodium (NaV) channels in a differentiated PC12 cell. Reprinted from Ref. 122 (A. E. Ondrus, H. D. Lee, S. Iwanaga, W. H. Parsons, B. M. Andresen, W. E. Moerner and J. Du Bois, *Chem. Biol.,* 2012, **19**, 902-912), with permission from Elsevier.

Figure 7 shows a few examples of super-resolution images. In Fig. 7a, *Caulobacter crescentus* cell surfaces are imaged far beyond the diffraction limit using a small-molecule photoactivatable rhodamine molecule, described in detail in Ref. [121]. The subdiffraction-sized cell stalks of various lengths are easily visualized. Figure 7b also shows *Caulobacter* cells, but now the cell surface has been imaged using PAINT and the Nile Red molecule, shown in gray. At the same time, a fiber made of CreS proteins has been imaged by fusion to EYFP, with light-induced blinking of the fluorescent proteins used as the active control mechanism. These images are actually three-dimensional images acquired using the double-helix point-spread function microscope described in Section 4, and the "double-helix" is sketched in an artist conception. The details of the imaging procedure are described in Ref. [123]. Finally in Fig. 7c, super-resolution and corresponding diffraction-limited images are shown for a differentiated PC12m neuronal model cell[122]. Here, a completely different active-control mechanism was used, where a fluorescent saxitoxin molecule was added to the buffer outside the cell. The diffusing neurotoxin binds to voltage-gated Na channels on the cell membrane, and the resulting flash of light from the bound fluorescent ligand in several imaging frames yields the images shown. From these few

examples, it is hoped that the breadth and variety of super-resolution imaging as a powerful tool for cell biology can be appreciated.

4. Three-dimensional localization microscopy

Although super-resolution localization microscopy of thin (~ two dimensional) samples has proven to be extremely informative, life happens in 3D: A cell (Or even a nucleus) is typically several microns thick, which is larger than the <1μm depth of focus of a high NA objective. As a result, with a standard microscope imaging a thick sample, a point source that is more than a few hundred nanometers away from the focal plane appears large, blurry ('defocused') and very dim.

Several schemes exist for adding axial (z) information to localization microscopy, thereby enabling 3D super-resolution imaging: multi-plane imaging[124-126], using a tilted mirror to generate a side view of the sample[127], single-photon interferometry[128] , and point-spread-function (PSF) engineering[129-137] . In the last case, the PSF of the microscope is altered by adding optical elements along the emission path, such that the shape of the acquired image of a single emitter (namely, the PSF) is indicative of the emitter's axial (z) position. PSF engineering for 3D imaging has the benefit of being a relatively simple method, requiring only a small number of optical elements that can be added to augment an existing standard microscope. Nevertheless the method exhibits extremely high precision, on the order of 10 nm in 3D for single-molecule localization for ~1000 photons detected, is scan-free, and has been recently extended to allow a very large, variable z-range, of up to 20 μm with a concomitant reduction in precision [137].

4.1 PSF Engineering

A general way to control the PSF of a microscope is to place an optical phase-changing element in a plane conjugate to the pupil plane, i.e. the Fourier plane of the microscope (Fig. 8)[129]. Since there is a Fourier transform relation between the pupil plane and the image plane, multiplying the electromagnetic field (originating from the emitter) by the complex transmission function of the pupil-plane phase element is equivalent to a convolution operation in the image plane[138]. This corresponds to modifying the PSF.

Various PSF designs have been used in recent years to encode z information (Fig. 8). These include an elliptical (astigmatic) PSF[130, 131], the rotating double-helix[132, 139], the phase-ramp[134], the accelerating-beam[135] and the saddle-point/Tetrapods[136, 137]. The different PSFs differ in the way they are produced, e.g. by using a cylindrical lens[131], a phase-ramp[134], or an especially designed phase-mask in the Fourier plane[132, 135-137]. However, their purpose is the same – to encode the axial position of the emitter by the shape of its image. Different PSFs have different characteristics, and their performance varies. For an example of the use of these ideas in cellular imaging, see Fig. 7b.

Two key parameters by which one can evaluate the applicability of a PSF to an experimental measurement are its precision and its applicable depth (z) range. The precision associated with a specific PSF means how well (how *precisely*) one can localize, i.e. determine the position of the emitter, by measuring its image (the PSF). Emitter localization is a parameter estimation problem: Given a noisy measurement (pixelated image of a PSF), and a known optical system and noise model – one must determine the 3D position of the emitter and possibly its brightness and background level (3-5 parameters)[136, 140]. As such, tools from information theory can be used in order to quantify the precision obtainable from a PSF.

A useful measure to evaluate the theoretical precision of a PSF, borrowed from information theory, is Fisher information[141, 142]. Fisher information is a mathematical measure of the sensitivity of an observable quantity (the PSF) to changes in its underlying parameters (emitter position). From the Fisher information function, one derives the Cramér-Rao lower bound (CRLB), which is the optimal (best) x, y, z precision that can be attained with any unbiased estimator. It has been shown that the CRLB can be approached in practice[98, 143, 144].

Fisher information analysis has been used to evaluate the effect of different imaging parameters on precision (e.g. pixel-size, multifocal vs. single plane imaging)[140, 145], to show that the double-helix PSF is more precise and uniform in z than astigmatism and bi-plane imaging over a ~3µm z-range[141], and to fine tune the double-helix design[146]. Importantly, treating Fisher information as a design variable (rather than an analysis metric) enables algorithmic and/or computational design of optimally precise PSFs. This has been recently achieved by solving an optimization problem of maximizing Fisher information for determination of x, y, and z subject to the system's constraints, including background noise. The resulting optimal PSFs are the

saddle-point[136], and more generally - Tetrapod PSFs[137].
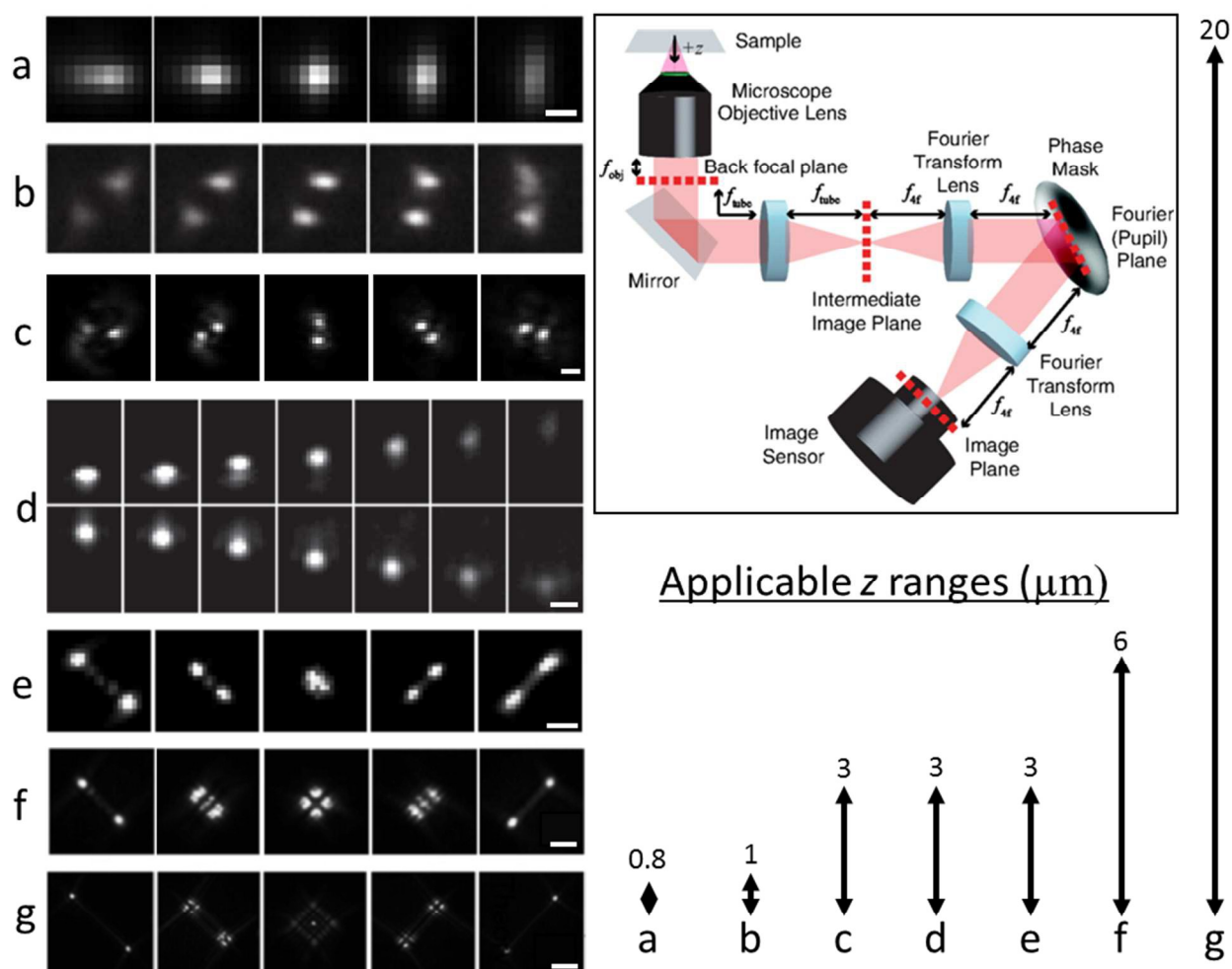
Figure 8. Various PSFs for 3D localization microscopy shown as a function of z-position of the emitter (experimentally measured). (a) Astigmatic[131]. Scale bar=~0.5µm. From Ref. 131 (B. Huang, W. Wang, M. Bates and X. Zhuang, *Science*, 2008, **319**, 810-813). Reprinted with permission from AAAS. (b) Phase-ramp[134]. Reprinted with kind permission from Springer Science and Business Media: Ref. 134 (D. Baddeley, M. B. Cannell and C. Soeller, *Nano Research,* 2011, **4**, 589-598). (c) Double-Helix[132]. Scale bar=2µm. Reprinted with permission from Ref. 132. (d) Accelerating beam[135]. Scale bar=1µm. Reprinted by permission from Macmillan Publishers Ltd: Nat. Photonics (S. Jia, J. C. Vaughan and X. Zhuang, *Nat. Photonics,* 2014, **8**, 302-306), copyright (2014) (e) Saddle-point[136]. Scale bar=1µm. Reprinted from Ref. 136, copyright (2014) by The American Physical Society. (f)+(g) Tetrapods[137], scale bars=2µm and 5µm, respectively. The arrows (right) represent the z-ranges over which the PSFs on the left were imaged, which correspond to their applicable depth ranges. Top right: Experimental setup for pupil plane modulation-based PSF engineering [136]. Adapted with permission from Ref. 137 (Y. Shechtman, L. E. Weiss, A. S. Backer, S. J. Sahl and W. E. Moerner, *Nano Lett.,* 2015, **15**, 4194-4199). Copyright (2015) American Chemical Society.

4.2 Single-molecule orientation

One specific consideration for single-molecule microscopy stems from the fact that single-molecules (with low rotational mobility) are not isotropic emitters, and the dipole nature of a single fluorophore can be non-negligible, and even informative[147-152]. A practical implication of the dipole nature of fluorophore emission is that the emitter's orientation may need to be taken into account when localizing single molecules from microscope images. Ignoring this effect can lead to localization errors: out-of-focus molecules can appear to be shifted in the lateral (x-y) plane, simply due to their non-isotropic emission profile[133, 153, 154].

One approach to handling dipole-induced localization bias is to measure the orientation of a fluorophore, and later correct for the localization error by post processing. The orientation can be determined by a variety of methods, ranging from the use of polarization optics[148, 149, 155] to analysis of the defocused emitter's image[150, 156]. An especially useful method to determine orientation is PSF engineering, which has the advantage of being simple, precise, and robust to minor defocus errors[129]. This can be achieved, for example, by using the Double-Helix PSF[133], a quadrated-pupil[157], or a bisected mask[158].

Alternatively, it has been recently suggested that PSF polarization engineering can be used to avoid dipole-induced localization bias by removing the effect of dipole orientation from the measurement itself[159]. This approach utilizes an azimuthal polarizer in the Fourier plane to remove transmitted light arising from the z component of the dipole moment, resulting in unbiased lateral localization determination, and experimental demonstrations of this idea are to be expected in the near future.

5. Single-molecule photodynamics and transport properties in solution

Single molecules are frequently used as sensors to probe nanoscale dynamics[160]. To obtain the most information from each molecule, it is highly desirable to observe the molecule for as long as possible in a non-perturbative environment. Although free diffusion-based measurements are routinely implemented and provide invaluable insight into problems such as protein folding[161], RNA polymerase-DNA interaction[162] and molecular aggregation[163], such methods are limited by Brownian motion to a per-molecule observation window of only ~1 ms, too short to observe dynamics of many biologically relevant processes.

The most commonly adopted remedy is to tether the molecule to a surface[164], but the act of immobilization could perturb the system of interest[165]. It is also possible to encapsulate single molecules in nano-containers to spatially limit Brownian motion for extended measurements[166-169]. Another approach is to directly follow the motion of a single molecule over long distances as it moves around, using feedback control. Many clever instruments have been designed around this scheme (Table 2). Although feedback tracking is particularly powerful in a cellular context to reveal the heterogeneous environment around a single-molecule probe, the slow mechanical

movement of a piezoelectric actuator currently limits the application of this approach to only slow-diffusing molecules.

Experiment	Reference
Orbital tracking in cells	170, 171
Confocal 3D tracking of single nanoparticles in solution	172, 173
3D orbital tracking of nanometer-sized objects	174-176
Non-scanning, bi-plane tracking of single nanoparticles in solution	177
3D tracking in cells using a tetrahedral arrangement of detection/excitation spots	178-180
Cellular uptake of a single nanoparticle	181

Table 2. Feedback tracking of single molecules in solution and cells.

An alternative approach is to "trap" a single molecule in solution, so it does not escape the field-of-view of observation. Note that the forces provided by optical tweezers are generally too weak to capture single biomolecules at reasonable laser intensities, so other forces have to be

Figure 9. The working principles of the ABEL trap: single-molecule motion in a microfluidic environment is tracked with high speed and Brownian motion is compensated by applying appropriate electrokinetic forces (black arrow) in 2D in a feedback loop. The motion of the molecule along the third dimension (z) is confined within the ~600 nm depth of the microfluidic chip (inset).
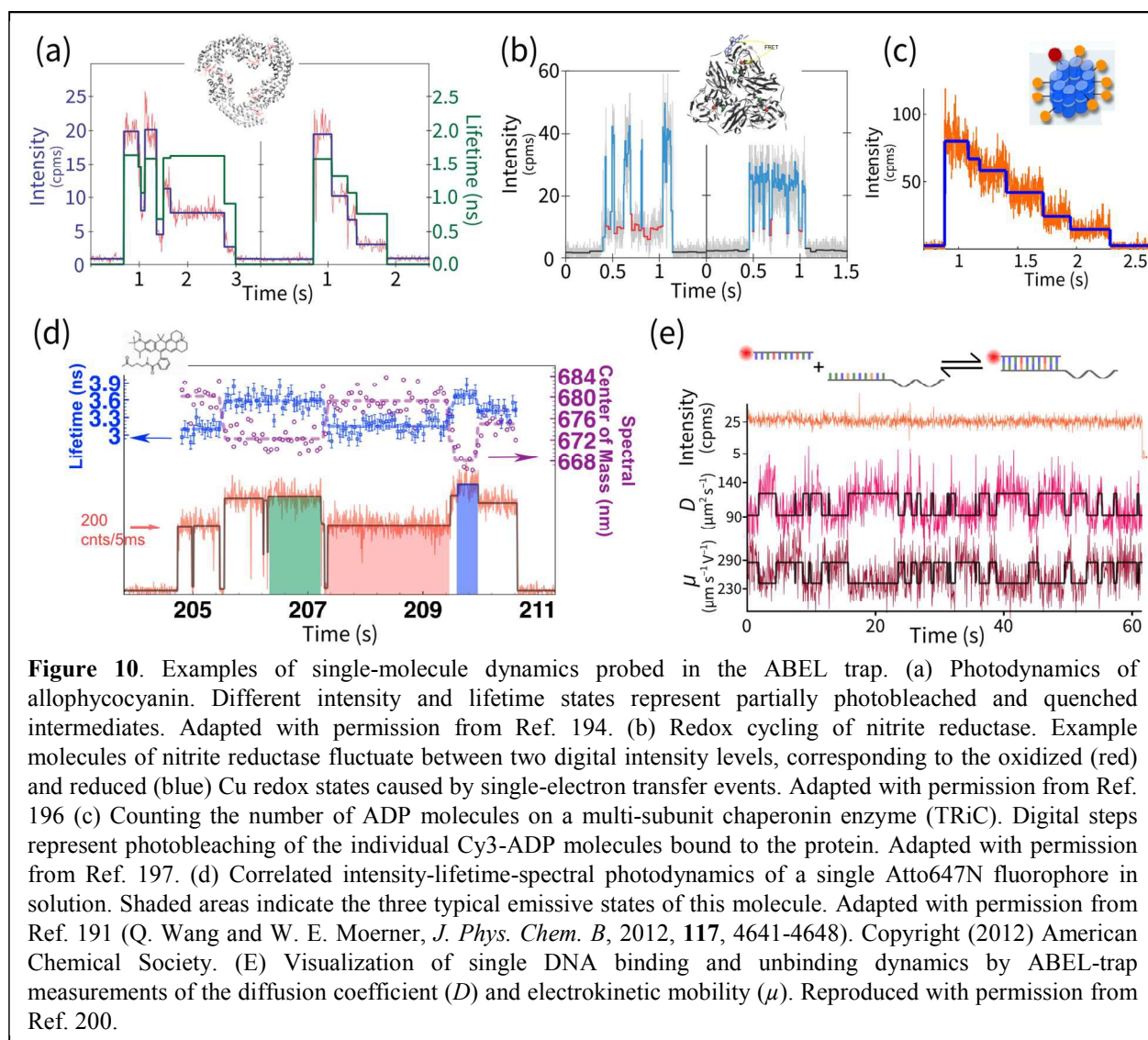
considered. The Anti-Brownian Electrokinetic (ABEL) trap has been developed for this purpose[182-184]. Unlike an optical trap, where the trapping force is provided by a physical potential, the ABEL trap uses feedback control to counteract Brownian motion. Its basic operating principle is extremely simple (Fig. 9): a high-speed imaging module continuously monitors the position of a single molecule and depending on where the molecule is, appropriate feedback voltages are applied in a microfluidic environment to drive electrokinetic motion that restores the molecule's position. In the ABEL trap, electrokinetic forces are utilized due to their favorable strength at the nanoscale and fast (~μs) response times.

Since its inception a decade ago[182], the ABEL trap has evolved from a proof-of-principle device to a reliable and versatile platform for single-molecule biophysics research. First-generation traps used fast EMCCD cameras and centroid fitting algorithms to determine position[185]. Later it was realized that the camera-based approach was too slow for trapping biomolecules and laser-scanning methods were subsequently implemented[186] to detect position. In the most advanced version of the trap, a focused laser spot undergoes a 32-point "knight's tour" scanning pattern at the sample plane at a speed of 600 ns per point, and every photon-stamped beam position is taken as an estimation of molecule position[187]. This photon-by-photon position sensing scheme, together with a real-time Kalman filter [188, 189] implemented on dedicated hardware to reduce measurement noise, greatly extended the trap's capability to capture molecules of the smallest scale. With the choice of a photostable label, single proteins and short strands of nucleic acids can be trapped for 10s of seconds, limited only by probe photobleaching. Even individual fluorophores, the smallest fluorescent objects, can be trapped

for a couple of seconds[190, 191]. More recently, other groups have implemented ABEL traps with unique capabilities such as trapping in all three dimensions[192] and feedback based on integrated RF circuits[193].

By feedback suppression of Brownian motion, the ABEL trap extends the observation time of a single biomolecule in solution by more than three orders of magnitude, permitting direct observation of nanoscale dynamics without immobilization. We have used the device to study

Figure 10. Examples of single-molecule dynamics probed in the ABEL trap. (a) Photodynamics of allophycocyanin. Different intensity and lifetime states represent partially photobleached and quenched intermediates. Adapted with permission from Ref. 194. (b) Redox cycling of nitrite reductase. Example molecules of nitrite reductase fluctuate between two digital intensity levels, corresponding to the oxidized (red) and reduced (blue) Cu redox states caused by single-electron transfer events. Adapted with permission from Ref. 196 (c) Counting the number of ADP molecules on a multi-subunit chaperonin enzyme (TRiC). Digital steps represent photobleaching of the individual Cy3-ADP molecules bound to the protein. Adapted with permission from Ref. 197. (d) Correlated intensity-lifetime-spectral photodynamics of a single Atto647N fluorophore in solution. Shaded areas indicate the three typical emissive states of this molecule. Adapted with permission from Ref. 191 (Q. Wang and W. E. Moerner, *J. Phys. Chem. B*, 2012, **117**, 4641-4648). Copyright (2012) American Chemical Society. (E) Visualization of single DNA binding and unbinding dynamics by ABEL-trap measurements of the diffusion coefficient (D) and electrokinetic mobility (μ). Reproduced with permission from Ref. 200.

the behaviors of a variety of biomolecules. In one of the first applications, we examined the photodynamics of single allophycocyanin proteins[194] (Fig. 10a), an important antenna complex in cyanobacteria. Correlated dynamics of fluorescence intensity and excited-state lifetime report on photobleaching processes and subtle structure-function relations of pigment-protein interactions. A more elaborated detection scheme with additional fluorescence parameters has been subsequently used to study other antenna complexes in nature[195] and the photophysics of

single fluorophores (Fig. 10d). As another example[196], an engineered FRET redox sensor was used to directly visualize the transitions between discrete redox states of the enzyme nitrite reductase (Fig. 10b), providing new insights into the mechanism of catalysis. In yet another experiment[197], the number of ADP molecules (each labeled with a fluorophore) bound to a chaperonin enzyme TRiC can be directly counted by enumerating the number of photobleaching steps for a single enzyme in the trap (Fig. 10c). Meanwhile, other groups have built their own ABEL traps to expand the application to broader areas, such as sensing the rotary motion of FoF1 ATPase[198], probing electron spin resonance of NV centers[193], and testing of Landauer's principle in statistical physics[199] as listed in Table 3.

Recently, we showed that it is possible to extract size and charge information from trapped single molecules[200]. This advance relies on statistical analysis of the molecule's residual motion in the trap to extract diffusive and electric-field-induced motion parameters. Knowledge of single-molecule transport properties opens up a variety of new sensing possibilities in fluorescence spectroscopy. For example, we demonstrated visualization of the size and charge fluctuations of a single DNA molecule as it binds and unbinds complementary strands in real time (Fig. 10e).

With the capability to observe single-molecule dynamics in solution for extended periods without perturbation and the unprecedented amount of both spectroscopic and transport information from each molecule, we envision the ABEL trap to become an essential tool in nanoscience and technology.

Experiment	Reference
DNA conformational dynamics	201
Photodynamics, photoprotection, pigment organization principles of photosynthetic antenna complexes	194, 202-205
Conformational dynamics of single G-Protein coupled receptors in solution	206
ATP binding stoichiometry of single multi-subunit enzymes	197
Redox cycling of single nitrite reductase enzymes	196
Test of Landauer's principle	199
Direct visualization of biomolecular interactions	200
Electron spin resonance of nitrogen-vacancy centers in a single nanodiamond in solution	193

Table 3. Application of the ABEL trap to study biomolecules, chemistry and physics

6. Conclusion and Outlook

At the present time, single-molecule spectroscopy and microscopy continue to have a broad impact across the sciences. Figure 11 illustrates some of the areas where these efforts have led to deeper insight. The advances in this area are the result of the dedicated work of many researchers all over the world, and the various papers presented during this Faraday Discussion provide a useful summary of many of the current areas of interest.
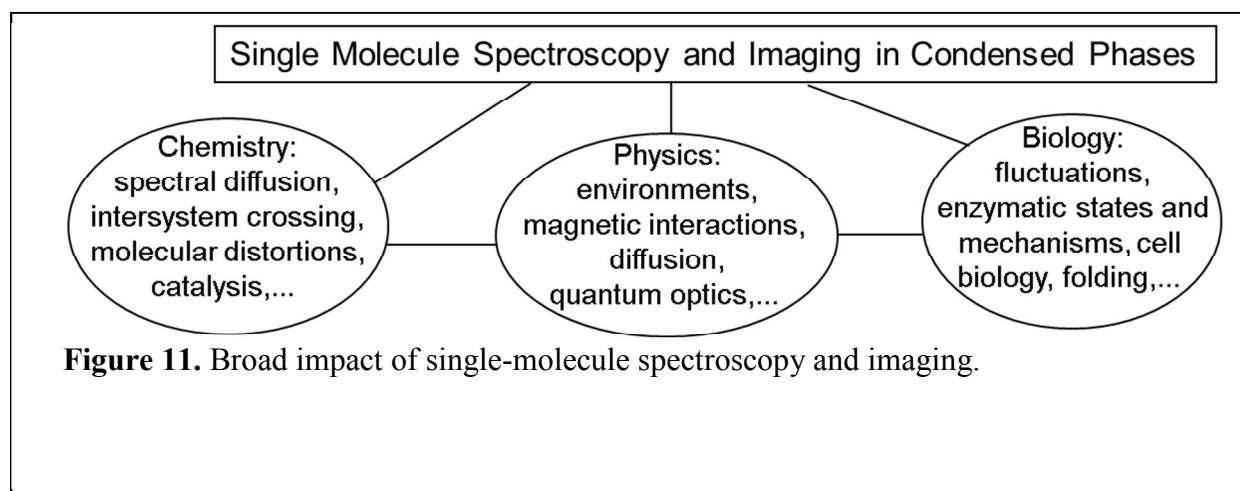
Figure 11. Broad impact of single-molecule spectroscopy and imaging.

Acknowledgements

Bibliography

1 W. E. Moerner and L. Kador, *Phys. Rev. Lett.,* 1989, **62**, 2535-2538.

2 W. E. Moerner and T. Basché, *Angew. Chem. Int. Ed.,* 1993, **105**, 537.

3 W. E. Moerner, *Science,* 1994, **265**, 46-53.

4 M. Orrit, J. Bernard, R. Brown and B. Lounis, *Prog. Optics,* 1996, **35**, 61-144.

5 T. Plakhotnik, E. A. Donley and U. P. Wild, *Annu. Rev. Phys. Chem.,* 1997, **48**, 181-212.

6 S. Nie and R. N. Zare, *Annu. Rev. Biophys. Biomol. Struct.,* 1997, **26**, 567-596.

7 W. E. Moerner and M. Orrit, *Science,* 1999, **283**, 1670-1676.

8 W. E. Moerner, *J. Phys. Chem. B,* 2002, **106**, 910-927.

9 W. E. Moerner and D. P. Fromm, *Rev. Sci. Instrum.,* 2003, **74**, 3597-3619.

10 P. Tinnefeld and M. Sauer, *Angew. Chem. Int. Ed.,* 2005, **44**, 2642-2671
(DOI:10.1002/anie.200300647).

11 P. V. Cornish and T. Ha, *ACS Chem. Biol.,* 2007, **2**, 53.

12 W. E. Moerner, P. J. Schuck, D. P. Fromm, A. Kinkhabwala, S. J. Lord, S. Y. Nishimura, K.
A. Willets, A. Sundaramurthy, G. S. Kino, M. He, Z. Lu and R. J. Twieg, in *in Single Molecules
and Nanotechnology,* ed. ed. R. Rigler and H. Vogel, Springer-Verlag, Berlin, 2008, pp.1-23.

13 T. Basché, W. E. Moerner, M. Orrit and U. P. Wild, Eds. *Single Molecule Optical Detection,
Imaging, and Spectroscopy* Verlag-Chemie, Munich, 1997.

14 C. Zander, J. Enderlein and R. A. Keller, Eds. *Single-Molecule Detection in Solution:
Methods and Applications*, Wiley-VCH, Berlin, 2002.

15 C. Gell, D. J. Brockwell and A. Smith, *Handbook of Single Molecule Fluorescence
Spectroscopy*, Oxford Univ. Press, Oxford, 2006.

16 P. R. Selvin and T. Ha, Eds. *Single-Molecule Techniques: A Laboratory Manual,* Cold Spring
Harbor Laboratory Press, Cold Spring Harbor, NY, 2008,.

17 E. Betzig, G. H. Patterson, R. Sougrat, O. W. Lindwasser, S. Olenych, J. S. Bonifacino, M.
W. Davidson, J. Lippincott-Schwartz and H. F. Hess, *Science,* 2006, **313**, 1642-1645.

18 M. J. Rust, M. Bates and X. Zhuang, *Nat. Methods,* 2006, **3**, 793-796.

19 S. T. Hess, T. P. K. Girirajan and M. D. Mason, *Biophys. J.,* 2006, **91**, 4258-4272.

20 A. M. Stoneham, *Rev. Mod. Phys.,* 1969, **41**, 82.

21 K. K. Rebane, *Impurity Spectra of Solids*, Plenum, New York, 1970.

22 K. K. Rebane, *Chem. Phys.,* 1994, **189**, 139-148.

23 R. I. Personov, E. I. Al'Shits and L. A. Bykovskaya, *Opt. Commun.,* 1972, **6**, 169-173 (DOI:http://dx.doi.org/10.1016/0030-4018(72)90220-9).

24 M. Orrit, J. Bernard and R. I. Personov, *J. Phys. Chem.,* 1993, **97**, 10256-10268.

25 H. de Vries and D. A. Wiersma, *J. Chem. Phys.,* 1979, **70**, 5807.

26 D. A. Wiersma, *Adv. Chem. Phys.,* 1981, **47**, 421.

27 M. Berg, C. A. Walsh, L. R. Narasimhan, K. A. Littau and M. D. Fayer, *J. Chem. Phys.,* 1988, **88**, 1564-1587 (DOI:http://dx.doi.org/10.1063/1.454136).

28 W. E. Moerner, Ed. *Topics in Current Physics 44; Persistent Spectral Hole-Burning: Science and Applications*, Springer, Berlin, 1988.

29 J. Friedrich and D. Haarer, *Angewandte Chemie International Edition in English,* 1984, **23**, 113-140 (DOI:10.1002/anie.198401131).

30 J. M. Hayes and G. J. Small, *Chemical Physics Letters,* 1978, **54**, 435-438 (DOI:http://dx.doi.org/10.1016/0009-2614(78)85255-5).

31 W. E. Moerner, *J. Molec. Electr.,* 1985, **1**, 55-71.

32 W. E. Moerner and M. D. Levenson, *J Opt Soc Am B,* 1985, **2**, 915-924 (DOI:10.1364/JOSAB.2.000915).

33 W. E. Moerner and T. P. Carter, *Phys. Rev. Lett.,* 1987, **59**, 2705.

34 T. P. Carter, M. Manavi and W. E. Moerner, *J. Chem. Phys.,* 1988, **89**, 1768.

35 G. C. Bjorklund, *Opt. Lett.,* 1980, **5**, 15.

36 T. P. Carter, D. E. Horne and W. E. Moerner, *Chem. Phys. Lett.,* 1988, **151**, 102.

37 L. Kador, D. E. Horne and W. E. Moerner, *J. Phys. Chem.,* 1990, **94**, 1237-1248.

38 E. A. Whittaker, M. Gehrtz and G. C. Bjorklund, *J. Opt. Soc. Am. B,* 1985, **2**, 1320.

39 M. Orrit and J. Bernard, *Phys. Rev. Lett.,* 1990, **65**, 2716-2719.

40 M. Orrit, J. Bernard, A. Zumbusch and R. I. Personov, *Chem. Phys. Lett.,* 1992, **196**, 595.

41 A. Zumbusch, L. Fleury, R. Brown, J. Bernard and M. Orrit, *Phys. Rev. Lett.,* 1993, **70**, 3584-3587.

42 F. Güttler, M. Croci, A. Renn and U. P. Wild, *Chem. Phys.,* 1996, **211**, 421-430.

43 W. E. Moerner, R. M. Dickson and D. J. Norris, *Adv.Atom.Molec.Opt.Phys.,* 1997, **38**, 193-236.

44 J. L. Skinner and W. E. Moerner, *J. Phys. Chem.,* 1996, **100**, 13251-13262.

45 W. E. Moerner, *Acc. Chem. Res.,* 1996, **29**, 563.

46 W. P. Ambrose and W. E. Moerner, *Nature,* 1991, **349**, 225-227.

47 W. P. Ambrose, T. Basché and W. E. Moerner, *J. Chem. Phys.,* 1991, **95**, 7150-7163.

48 T. Basché, W. E. Moerner, M. Orrit and H. Talon, *Phys. Rev. Lett.,* 1992, **69**, 1516-1519.

49 P. Tchénio, A. B. Myers and W. E. Moerner, *J. Phys. Chem.,* 1993, **97**, 2491.

50 P. Tchénio, A. B. Myers and W. E. Moerner, *Chem. Phys. Lett.,* 1993, **213**, 325.

51 A. B. Myers, P. Tchénio, M. Zgierski and W. E. Moerner, *J. Phys. Chem.,* 1994, **98**, 10377.

52 J. Köhler, J. A. J. M. Disselhorst, M. C. J. M. Donckers, E. J. J. Groenen, J. Schmidt and W. E. Moerner, *Nature,* 1993, **363**, 242-244.

53 W. E. Moerner, T. Plakhotnik, T. Irngartinger, U. P. Wild, D. Pohl and B. Hecht, *Phys. Rev. Lett.,* 1994, **73**, 2764.

54 W. E. Moerner and W. P. Ambrose, *Phys. Rev. Lett.,* 1991, **66**, 1376.

55 J. Friedrich and D. Haarer, in *Optical Spectroscopy of Glasses,* ed. I. Zschokke, Reidel, Dordrecht, 1986, pp.149.

56 P. D. Reilly and J. L. Skinner, *Phys. Rev. Lett.,* 1993, **71**, 4257-4260.

57 P. D. Reilly and J. L. Skinner, *J. Chem. Phys.,* 1995, **102**, 1540.

58 E. Geva and J. L. Skinner, *J. Phys. Chem. B,* 1997, **101**, 8920-8932.

59 T. Plakhotnik, W. E. Moerner, T. Irngartinger and U. P. Wild, *Chimia,* 1994, **48**, 31.

60 T. Basché and W. E. Moerner, *Nature,* 1992, **355**, 335-337.

61 T. Basché, W. P. Ambrose and W. E. Moerner, *J. Opt. Soc. Am. B,* 1992, **9**, 829.

62 D. Magde, E. Elson and W. W. Webb, *Phys. Rev. Lett.,* 1972, **29**, 705.

63 E. L. Elson and D. Magde, *Biopolymers,* 1974, **13**, 1-27.

64 D. L. Magde, E. L. Elson and W. W. Webb, *Biopolymers,* 1974, **13**, 29-61.

65 D. Magde, W. W. Webb and E. L. Elson, *Biopolymers,* 1978, **17**, 361-367.

66 M. Ehrenberg and R. Rigler, *Chem. Phys.,* 1974, **4**, 390-401 (DOI:http://dx.doi.org/10.1016/0301-0104(74)85005-6).

67 S. R. Aragón and R. Pecora, *J. Chem. Phys.,* 1976, **64**, 1791-1803 (DOI:http://dx.doi.org/10.1063/1.432357).

68 R. Rigler and J. Widengren, 1990, Proceedings of Bioscience 3, 180-183.

69 K. Peck, L. Stryer, A. N. Glazer and R. A. Mathies, *Proc. Natl. Acad. Sci. U. S. A.,* 1989, **86**, 4087-4091.

70 E. B. Shera, N. K. Seitzinger, L. M. Davis, R. A. Keller and S. A. Soper, *Chem. Phys. Lett.,* 1990, **174**, 553-557.

71 S. Nie, D. T. Chiu and R. N. Zare, *Science,* 1994, **266**, 1018-1021.

72 T. Hirschfeld, *Appl. Opt.,* 1976, **15**, 2965-2966 (DOI:10.1364/AO.15.002965).

73 E. Betzig and R. J. Chichester, *Science,* 1993, **262**, 1422-1425.

74 W. P. Ambrose, P. M. Goodwin, J. C. Martin and R. A. Keller, *Phys. Rev. Lett.,* 1994, **72**, 160-163.

75 X. S. Xie and R. C. Dunn, *Science,* 1994, **265**, 361-364.

76 J. J. Macklin, J. K. Trautman, T. D. Harris and L. E. Brus, *Science,* 1996, **272**, 255-258.

77 T. Funatsu, Y. Harada, M. Tokunaga, K. Saito and T. Yanagida, *Nature,* 1995, **374**, 555-559.

78 T. Schmidt, G. J. Schutz, W. Baumgartner, H. J. Gruber and H. Schindler, *Proc. Natl. Acad. Sci. U. S. A.,* 1996, **93**, 2926-2929.

79 R. Rigler and E. Elson, Eds. *Fluorescence Correlation Spectroscopy, Theory and Applications,* Springer, Berlin, 2001.

80 P. Schwille, *Cell Biochem. Biophys.,* 2001, **34**, 383-408.

81 S. T. Hess, S. Huang, A. A. Heikal and W. W. Webb, *Biochemistry,* 2002, **41**, 697-705.

30

82 S. Weiss, *Science,* 1999, **283**, 1676-1683.

83 W. E. Moerner, in *Single Molecule Spectroscopy in Chemistry, Physics and Biology: Nobel Symposium 138 Proceedings,* eds. A. Graslund, R. Rigler and J. Widengren, Springer-Verlag, Berlin, 2009, pp.25-60.

84 R. Rigler, M. Orrit and T. Basche, Eds. *Single Molecule Spectroscopy, Nobel Conference Lectures,* Springer-Verlag, Berlin, 2001.

85 A. Gräslund, R. Rigler and J. Widengren, Eds. *Single Molecule Spectroscopy in Chemistry, Physics and Biology: Nobel Symposium 138 Proceedings,* Springer-Verlag, Berlin, 2009.

86 R. M. Dickson, A. B. Cubitt, R. Y. Tsien and W. E. Moerner, *Nature,* 1997, **388**, 355-358.

87 R. Ando, H. Hama, M. Yamamoto-Hino, H. Mizuno and A. Miyawaki, *Proc. Natl. Acad. Sci. U. S. A.,* 2002, **99**, 12651-12656.

88 G. H. Patterson and J. Lippincott-Schwartz, *Science,* 2002, **297**, 1873-1877.

89 J. Wiedenmann, S. Ivanchenko, F. Oswald, F. Schmitt, C. Röcker, A. Salih, K. Spindler and G. U. Nienhaus, *Proc. Natl. Acad. Sci. U. S. A.,* 2004, **101**, 15905-15910 (DOI:10.1073/pnas.0403668101).

90 R. Ando, H. Mizuno and A. Miyawaki, *Science,* 2004, **306**, 1370-1373.

91 M. Ormo, A. B. Cubitt, K. Kallio, L. A. Gross, R. Y. Tsien and S. J. Remington, *Science,* 1996, **273**, 1392-1395.

92 J. S. Biteen, M. A. Thompson, N. K. Tselentis, G. R. Bowman, L. Shapiro and W. E. Moerner, *Nat. Methods,* 2008, **5**, 947-949.

93 E. Abbe, *Arch. Mikroskop. Anat.,* 1873, **9**, 413-468.

94 S. W. Hell, *Science,* 2007, **316**, 1153-1158 (DOI:10.1126/science.1137395).

95 M. G. L. Gustafsson, *J. Microsc.,* 2000, **198**, 82-87.

96 R. E. Thompson, D. R. Larson and W. W. Webb, *Biophys. J.,* 2002, **82**, 2775-2783.

97 X. Michalet and S. Weiss, *Proc. Natl. Acad. Sci. U. S. A.,* 2006, **103**, 4797-4798.

98 K. I. Mortensen, L. S. Churchman, J. A. Spudich and H. Flyvbjerg, *Nat. Methods,* 2010, **7**, 377-381.

99 N. Bobroff, *Rev. Sci. Instrum.,* 1986, **57**, 1152-1157.

100 L. S. Barak and W. W. Webb, *J. Cell Biol.,* 1982, **95**, 846-852.

101 J. Gelles, B. J. Schnapp and M. P. Sheetz, *Nature,* 1988, **331**, 450-453.

102 W. E. Moerner, *Rev Mod Phys,* 2015, **87**, 1183-1212 (DOI:10.1103/RevModPhys.87.1183).

103 A. Sharonov and R. M. Hochstrasser, *Proc. Natl. Acad. Sci. U. S. A.,* 2006, **103**, 18911-18916.

104 E. Mei, F. Gao and R. M. Hochstrasser, *Phys. Chem. Chem. Phys.,* 2006, **8**, 2077-2082.

105 M. Heilemann, S. van de Linde, M. Schüttpelz, R. Kasper, B. Seefeldt, A. Mukherjee, P. Tinnefeld and M. Sauer, *Angew. Chem. Int. Ed.,* 2008, **47**, 6172-6176 (DOI:10.1002/anie.200802376).

106 I. Testa, C. A. Wurm, R. Medda, E. Rothermel, C. von Middendorf, J. Foelling, S. Jakobs, A. Schoenle, S. W. Hell and C. Eggeling, *Biophys. J.,* 2010, **99**, 2686-2694.

107 T. Cordes, M. Strackharn, S. W. Stahl, W. Summerer, C. Steinhauer, C. Forthmann, E. M. Puchner, J. Vogelsang, H. E. Gaub and P. Tinnefeld, *Nano Lett.,* 2010, **10**, 645-651 (DOI:10.1021/nl903730r).

108 P. Lemmer, M. Gunkel, D. Baddeley, R. Kaufmann, A. Urich, Y. Weiland, J. Reymann, P. Mueller, M. Hausmann and C. Cremer, *Appl. Phys. B,* 2008, **93**, 1-12 (DOI:10.1007/s00340-008-3152-x).

109 H. D. Lee, S. J. Lord, S. Iwanaga, K. Zhan, H. Xie, J. C. Williams, H. Wang, G. R. Bowman, E. D. Goley, L. Shapiro, R. J. Twieg, J. Rao and W. E. Moerner, *J. Am. Chem. Soc.,* 2010, **132**, 15099-15101 (DOI:10.1021/ja1044192).

110 M. K. Lee, J. Williams, R. J. Twieg, J. Rao and W. E. Moerner, *Chem. Sci.,* 2013, **4**, 220-225 (DOI:10.1039/c2sc21074f).

111 F. Huang, T. M. P. Hartwich, F. E. Rivera-Molina, Y. Lin, W. C. Duim, J. J. Long, P. D. Uchil, J. R. Myers, M. A. Baird, W. Mothes, M. W. Davidson, D. Toomre and J. Bewersdorf, *Nat. Methods,* 2013, **10**, 653-658 (DOI:10.1038/NMETH.2488).

112 B. Huang, H. Babcock and X. Zhuang, *Cell,* 2010, **143**, 1047-1058.

113 M. A. Thompson, M. D. Lew and W. E. Moerner, *Annu. Rev. Biophys.,* 2012, **41**, 321-342 (DOI:10.1146/annurev-biophys-050511-102250).

114 M. A. Thompson, J. S. Biteen, S. J. Lord, N. R. Conley and W. E. Moerner, *Meth. Enzymol.,* 2010, **475**, 27-59.

115 J. S. Biteen and W. E. Moerner, *Cold Spring Harb. Perspect. Biol.,* 2010, **2**, a000448.

116 M. D. Lew, S. F. Lee, M. A. Thompson, H. D. Lee and W. E. Moerner, "Single-Molecule Photocontrol and Nanoscopy," in *Far-Field Optical Nanoscopy*, P. Tinnefeld, C. Eggeling, S. W. Hell, Eds., Springer, Berlin, Heidelberg, 2012, pp.1-24.

117 W. E. Moerner, *J. Microsc.,* 2012, **246**, 213-220.

118 A. Gahlmann, J. L. Ptacin, G. Grover, S. Quirin, A. R. S. von Diezmann, M. K. Lee, M. P. Backlund, L. Shapiro, R. Piestun and W. E. Moerner, *Nano Lett.,* 2013, **13**, 987-993 (DOI:10.1021/nl304071h).

119 S. J. Sahl and W. E. Moerner, *Curr. Opin. Struct. Biol.,* 2013, **23**, 778-787 (DOI:http://dx.doi.org/10.1016/j.sbi.2013.07.010).

120 A. Godin, B. Lounis and L. Cognet, *Biophys. J.,* 2014, **107**, 1777-1784 (DOI:http://dx.doi.org/10.1016/j.bpj.2014.08.028).

121 M. K. Lee, P. Rai, J. Williams, R. J. Twieg and W. E. Moerner, *J. Am. Chem. Soc.,* 2014, **136**, 14003-14006 (DOI:10.1021/ja508028h).

122 A. E. Ondrus, H. D. Lee, S. Iwanaga, W. H. Parsons, B. M. Andresen, W. E. Moerner and J. Du Bois, *Chem. Biol.,* 2012, **19**, 902-912 (DOI:10.1016/j.chembiol.2012.05.021).

123 M. D. Lew, S. F. Lee, J. L. Ptacin, M. K. Lee, R. J. Twieg, L. Shapiro and W. E. Moerner, *Proc. Natl. Acad. Sci. U. S. A.,* 2011, **108**, E1102-E1110 (DOI:10.1073/pnas.1114444108).

124 E. Toprak, H. Balci, B. H. Blehm and P. R. Selvin, *Nano Letters,* 2007, **7**, 2043-2045.

125 M. F. Juette, T. J. Gould, M. D. Lessard, M. J. Mlodzianoski, B. S. Nagpure, B. T. Bennett, S. T. Hess and J. Bewersdorf, *Nat. Methods,* 2008, **5**, 527-529.

126 P. Prabhat, S. Ram, E. S. Ward and R. J. Ober, *IEEE Trans. Nanobioscience,* 2004, **3**, 237-242.

127 J. Tang, J. Akerboom, A. Vaziri, L. L. Looger and C. V. Shank, *Proc. Natl. Acad. Sci. U. S. A.,* 2010, **107**, 10068-10073 (DOI:10.1073/pnas.1004899107).

128 G. Shtengel, J. A. Galbraith, C. G. Galbraith, J. Lippincott-Schwartz, J. M. Gillette, S. Manley, R. Sougrat, C. M. Waterman, P. Kanchanawong, M. W. Davidson, R. D. Fetter and H. F. Hess, *Proc. Natl. Acad. Sci. U. S. A.,* 2009, **106**, 3125-3130 (DOI:10.1073/pnas.0813131106).

129 A. S. Backer and W. E. Moerner, *J. Phys. Chem. B,* 2014, **118**, 8313-8329.

130 L. Holtzer, T. Meckel and T. Schmidt, *Appl. Phys. Lett.,* 2007, **90**, 053902.

131 B. Huang, W. Wang, M. Bates and X. Zhuang, *Science,* 2008, **319**, 810-813.

132 S. R. P. Pavani, M. A. Thompson, J. S. Biteen, S. J. Lord, N. Liu, R. J. Twieg, R. Piestun and W. E. Moerner, *Proc. Natl. Acad. Sci. U. S. A.,* 2009, **106**, 2995-2999 (DOI:10.1073/pnas.0900245106).

133 M. P. Backlund, M. D. Lew, A. S. Backer, S. J. Sahl, G. Grover, A. Agrawal, R. Piestun and W. E. Moerner, *Proc. Natl. Acad. Sci. U. S. A.,* 2012, **109**, 19087-19092 (DOI:10.1073/pnas.1216687109).

134 D. Baddeley, M. B. Cannell and C. Soeller, *Nano Research,* 2011, **4**, 589-598.

135 S. Jia, J. C. Vaughan and X. Zhuang, *Nat. Photonics,* 2014, **8**, 302-306.

136 Y. Shechtman, S. J. Sahl, A. S. Backer and W. E. Moerner, *Phys. Rev. Lett.,* 2014, **113**, 133902.

137 Y. Shechtman, L. E. Weiss, A. S. Backer, S. J. Sahl and W. E. Moerner, *Nano Lett.,* 2015, **15**, 4194-4199 (DOI:10.1021/acs.nanolett.5b01396).

138 J. W. Goodman, *Introduction to Fourier Optics*, Roberts & Company Publishers, Greenwood Village, CO, 2005.

139 R. Piestun, Y. Y. Schechner and J. Shamir, *J. Opt. Soc. Am. A,* 2000, **17**, 294-303.

140 R. J. Ober, S. Ram and E. S. Ward, *Biophys. J.,* 2004, **86**, 1185-1200.

141 M. Badieirostami, M. D. Lew, M. A. Thompson and W. E. Moerner, *Appl. Phys. Lett.,* 2010, **97**, 161103 (DOI:10.1063/1.3499652).

142 S. M. Kay, *Fundamentals of Statistical Signal Processing: Estimation Theory*, Prentice-Hall PTR, Englewood Cliffs, NJ, 1993.

143 A. V. Abraham, S. Ram, J. Chao, E. S. Ward and R. J. Ober, *Opt. Express,* 2009, **17**, 23352-23373.

144 C. S. Smith, N. Joseph, B. Rieger and K. A. Lidke, *Nat. Methods,* 2010, **7**, 373-375.

145 S. Ram, P. Prabhat, J. Chao, E. S. Ward and R. J. Ober, *Biophys. J.,* 2008, **95**, 6025-6043.

146 G. Grover, K. DeLuca, S. Quirin, J. DeLuca and R. Piestun, *Opt. Express,* 2012, **20**, 26681.

147 T. Ha, T. Enderle, D. S. Chemla, P. R. Selvin and S. Weiss, *Phys. Rev. Lett.,* 1996, **77**, 3979-3972.

148 J. N. Forkey, M. E. Quinlan and Y. E. Goldman, *Biophys. J.,* 2005, **89**, 1261-1271 (DOI:DOI: 10.1529/biophysj.104.053470).

149 S. A. Rosenberg, M. E. Quinlan, J. N. Forkey and Y. E. Goldman, *Acc. Chem. Res.,* 2005, **38**, 583-593.

150 E. Toprak, J. Enderlein, S. Syed, S. A. McKinney, R. G. Petschek, T. Ha, Y. E. Goldman and P. R. Selvin, *Proc. Natl. Acad. Sci. U. S. A.,* 2006, **103**, 6495-6499.

151 D. Axelrod, *Methods Cell Biol.,* 1989, **30**, 333-352.

152 E. J. Peterman, H. Sosa and W. E. Moerner, *Annu. Rev. Phys. Chem.,* 2004, **55**, 79-96.

153 J. Enderlein, E. Toprak and P. R. Selvin, *Opt. Express,* 2006, **14**, 8111-8120 (DOI:10.1364/OE.14.008111).

154 J. Engelhardt, J. Keller, P. Hoyer, M. Reuss, T. Staudt and S. W. Hell, *Nano Lett.,* 2011, **11**, 209-213 (DOI:10.1021/nl103472b).

155 J. T. Fourkas, *Opt. Lett.,* 2001, **26**, 211-213.

156 M. Böhmer and J. Enderlein, *J. Opt. Soc. Am. B,* 2003, **20**, 554-559.

157 A. S. Backer, M. P. Backlund, M. D. Lew and W. E. Moerner, *Opt. Lett.,* 2013, **38**, 1521-1523.

158 A. S. Backer, M. P. Backlund, A. R. Diezmann, S. J. Sahl and W. E. Moerner, *Appl. Phys. Lett.,* 2014, **104**, 193701-193705.

159 M. D. Lew and W. E. Moerner, *Nano Lett.,* 2014, **14**, 6407-6413.

160 C. Joo, H. Balci, Y. Ishitsuka, C. Buranachai and T. Ha, *Annu. Rev. Biochem.,* 2008, **77**, 51-76.

161 B. Schuler, E. A. Lipman and W. A. Eaton, *Nature,* 2002, **419**, 743-747.

162 A. N. Kapanidis, E. Margeat, S. O. Ho, E. Kortkhonjia, S. Weiss and R. H. Ebright, *Science,* 2006, **314**, 1144-1147 (DOI:10.1126/science.1131399).

163 A. Orte, N. R. Birkett, R. W. Clarke, G. L. Devlin, C. M. Dobson and D. Klenerman, *Proc. Natl. Acad. Sci. U. S. A.,* 2008, **105**, 14424-14429 (DOI:10.1073/pnas.0803086105).

164 S. D. Chandradoss, A. D. Haagsma, Y. K. Lee, J. -. Hwang, J. -. Nam and C. Joo, *J. Vis. Exp.,* 2014, **86**, e50549.

165 M. Friedel, A. Baumketner and J. E. Shea, *Proc. Natl. Acad. Sci. U. S. A.,* 2006, **103**, 8396-8401 (DOI:10.1073/pnas.0601210103 ER).

35

166 I. Cisse, B. Okumus, C. Joo and T. Ha, *Proc. Natl. Acad. Sci. U. S. A.,* 2007, **104**, 12646-12650.

167 M. J. Shon and A. E. Cohen, *J. Am. Chem. Soc.,* 2012, **134**, 14618-14623.

168 H. H. Gorris, D. M. Rissin and R. W. David, *Proc. Natl. Acad. Sci. U. S. A.,* 2007, **104**, 17680-17685.

169 Y. Rondelez, G. Tresset, T. Nakashima, Y. Kato-Yamada, H. Fujita, S. Takeuchi and H. Noji, *Nature,* 2005, **433**, 773-777.

170 V. Levi, Q. Q. Ruan and E. Gratton, *Biophys. J.,* 2005, **88**, 2919-2928.

171 Y. Katayama, O. Burkacky, M. Meyer, C. Bräuchle, E. Gratton and D. C. Lamb, *ChemPhysChem,* 2009, **10**, 2458-2464.

172 H. Cang, C. M. Wong, C. S. Xu, A. H. Rizvi and H. Yang, *Appl. Phys. Lett.,* 2006, **88**, 223901.

173 H. Cang, C. S. Xu, D. Montiel and H. Yang, *Opt. Lett.,* 2007, **32**, 2729-2731.

174 K. McHale, A. J. Berglund and H. Mabuchi, *Nano Lett.,* 2007, **7**, 3535-3539 (DOI:10.1021/nl0723376).

175 K. McHale and H. Mabuchi, *J. Am. Chem. Soc.,* 2009, **131**, 17901-17907.

176 D. Ernst, S. Hain and J. Koehler, *J. Opt. Soc. Am. A,* 2012, **29**, 1277-1287.

177 M. F. Juette and J. Bewersdorf, *Nano Lett.,* 2010, **10**, 4657-4663.

178 G. A. Lessard, P. M. Goodwin and J. H. Werner, *Appl. Phys. Lett.,* 2007, **91**, 224106-3.

179 N. P. Wells, G. A. Lessard, P. M. Goodwin, M. E. Phipps, P. J. Cutler, D. S. Lidke, B. S. Wilson and J. H. Werner, *Nano Lett.,* 2010, **10**, 4732-4737.

180 E. P. Perillo, Y. -. Liu, K. Huynh, C. Liu, C. -. Chou, M. -. Hung, H. -. Yeh and A. K. Dunn, *Nat. Commun.,* 2015, **6**, 7874.

181 K. Welsher and H. Yang, *Nature nanotechnology,* 2014, **9**, 198-203.

182 A. E. Cohen and W. E. Moerner, *Appl. Phys. Lett.,* 2005, **86**, 093109.

183 A. E. Cohen and W. E. Moerner, *Proc. Natl. Acad. Sci. U. S. A.,* 2006, **103**, 4362-4365.

184 Q. Wang, R. H. Goldsmith, Y. Jiang, S. D. Bockenhauer and W. E. Moerner, *Acc. Chem. Res.,* 2012, **45**, 1955-1964 (DOI:10.1021/ar200304t).

185 A. E. Cohen and W. E. Moerner, *Proc. SPIE,* 2005, **5699**, 296-305.

186 A. E. Cohen and W. E. Moerner, *Opt. Express,* 2008, **16**, 6941-6956.

187 Q. Wang and W. E. Moerner, *ACS Nano,* 2011, **5**, 5792-5799.

188 Q. Wang and W. E. Moerner, *Appl. Phys. B,* 2010, **99**, 23-30.

189 A. P. Fields and A. E. Cohen, *Opt. Express,* 2012, **20**, 22589-22601.

190 A. P. Fields and A. E. Cohen, *Proc. Natl. Acad. Sci. U. S. A.,* 2011, **108**, 8937-8942.

191 Q. Wang and W. E. Moerner, *J. Phys. Chem. B,* 2012, **117**, 4641-4648.

192 J. K. King, B. K. Canfield and L. M. Davis, *Appl. Phys. Lett.,* 2013, **103** (DOI:http://dx.doi.org/10.1063/1.4816325).

193 M. Kayci, H. -. Chang and A. Radenovic, *Nano Lett.,* 2014, **14**, 5335-5341.

194 R. H. Goldsmith and W. E. Moerner, *Nat. Chem.,* 2010, **2**, 179-186 (DOI:10.1038/NCHEM.545 ER).

195 G. S. Schlau-Cohen, S. Bockenhauer, Q. Wang and W. E. Moerner, *Chem. Sci.,* 2014, **5**, 2933-2939.

196 R. H. Goldsmith, L. C. Tabares, D. Kostrz, C. Dennison, T. J. Aartsma, G. W. Canters and W. E. Moerner, *Proc. Natl. Acad. Sci. U. S. A.,* 2011, **108**, 17269-17274.

197 Y. Jiang, N. R. Douglas, N. R. Conley, E. J. Miller, J. Frydman and W. E. Moerner, *Proc. Natl. Acad. Sci. U. S. A.,* 2011, **108**, 16962-16967.

198 B. Su, M. G. Düser, N. Zarrabi, T. Heitkamp, I. Ilka Starke and M. Börsch, *Proc. SPIE,* 2015, **9329**.

199 Y. Jun, M. Gavrilov and J. Bechhoefer, *Phys. Rev. Lett.,* 2014, **113**, 190601.

200 Q. Wang and W. E. Moerner, *Nat. Methods,* 2014, **11**, 555-558.

201 A. E. Cohen and W. E. Moerner, *Proc. Natl. Acad. Sci. U. S. A.,* 2007, **104**, 12622-12627 (DOI:10.1073/pnas.0610396104 ER).

202 G. S. Schlau-Cohen, Q. Wang, J. Southall, R. J. Cogdell and W. E. Moerner, *Proc. Natl. Acad. Sci. U. S. A.,* 2013, **110**, 10899-10903.

203 G. Schlau-Cohen, H. Yang, T. P. J. Krueger, P. Xu, M. Gwizdala, R. van Grondelle, R. Croce and W. E. Moerner, *J. Phys. Chem. Lett.,* 2015, **6**, 860-867 (DOI:10.1021/acs.jpclett.5b00034).

204 Q. Wang and W. E. Moerner, *Proc. Natl. Acad. Sci. U. S. A.,* 2015, published online October 5, 2015 (DOI:10.1073/pnas.1514027112).

205 S. Bockenhauer and W. E. Moerner, *J. Phys. Chem. A,* 2013, **117**, 8399-8406.

206 S. Bockenhauer, A. Fuerstenberg, J. Y. Yao, B. K. Kobilka and W. E. Moerner, *J. Phys. Chem. B,* 2011, **115**, 13328-13338.